Trajectory Optimization for Cellular-Connected UAV Under Outage Duration Constraint

Shuowen Zhang, *Member, IEEE* and Rui Zhang, *Fellow, IEEE*

Abstract

Enabling cellular access for unmanned aerial vehicles (UAVs) is a practically appealing solution to realize their high-quality communications with the ground for ensuring safe and efficient operations. In this paper, we study the trajectory design for a cellular-connected UAV that needs to fly from given initial to final locations, while communicating with the ground base stations (GBSs) subject to a minimum signal-to-noise ratio (SNR) requirement along its flight. However, due to various practical considerations such as GBSs' locations and coverage range as well as UAV's trajectory and mobility constraints, the SNR target may not be met at certain time periods during the flight, each termed as an *outage duration*. In this paper, we first propose a general *outage cost function* in terms of outage durations in the flight, which includes the two commonly used metrics, namely total outage duration and maximum outage duration as special cases. Based on it, we formulate a UAV trajectory optimization problem to minimize its mission completion time, subject to a constraint on the maximum tolerable outage cost. To tackle this challenging (non-convex) optimization problem, we first transform it into a tractable form and thereby reveal some useful properties of the optimal trajectory solution. Based on these properties, we further simplify the problem and propose efficient algorithms to check its feasibility and obtain optimal as well as low-complexity suboptimal solutions for it by leveraging graph theory and convex optimization techniques. Numerical results show that our proposed trajectory designs outperform that by the conventional method of dynamic programming, in terms of both performance and complexity.

Index Terms

UAV communication, cellular network, trajectory optimization, outage duration, graph theory, Lagrange relaxation, dynamic programming.

This work has been submitted in part to the IEEE International Conference on Communications (ICC), Shanghai, China, May 20-24, 2019.

The authors are with the Department of Electrical and Computer Engineering, National University of Singapore (e-mails: {elezhsh;elezhang}@nus.edu.sg).

I. Introduction

Unmanned aerial vehicles (UAVs), or namely drones, have recently drawn significant attention due to its various promising applications such as cargo delivery, aerial inspection, video streaming, emergency response, etc [1]. With the dramatically increasing demand for UAVs, it is of paramount importance to ensure that all UAVs can operate safely and efficiently, which calls for high-quality communications between UAVs and their ground pilots/users. They generally include ultra-reliable and secure control and non-payload communications (CNPC) to exchange critical control and command (C&C) messages with the ground, as well as high-rate payload communications to deliver the information collected/captured by the UAV (e.g., high-resolution videos/images) to the ground [1]. A new and cost-effective solution to achieve the above goal is *cellular-enabled UAV communication*, where the ground base stations (GBSs) in the cellular network are used to communicate with UAVs by treating them as a new type of *aerial users* [1]–[11]. Compared to the traditional point-to-point UAV-ground communications via Wi-Fi over the unlicensed spectrum which are restricted to the visual line-of-sight (VLoS) range, cellular-enabled UAV communication supports beyond VLoS (BVLoS) UAV operation, and is expected to achieve significant performance enhancement by exploiting the high-speed backhaul links in the cellular network [1].

Compared to traditional terrestrial users, UAVs have drastically different channel characteristics with their serving GBSs, which give rise to both challenges and opportunities in the design of cellular-enabled UAV communications [1]. Specifically, the communication channels between UAVs and GBSs are generally dominated by the line-of-sight (LoS) paths [4], which lead to a pronounced macro-diversity gain in associating UAVs with potentially more GBSs with strong LoS channels as compared to the terrestrial users. However, on the other hand, LoS channels also incur severe interference with the non-associated GBSs. To resolve this issue, effective air-ground interference management techniques need to be devised [5]–[9]. For example, in [6], [7], a UAV user with multiple antennas in the cellular uplink was considered, and a multi-beam transmission scheme was proposed to enhance the communication performance via transmit beamforming design. To suppress the aerial interference caused to terrestrial communications, a novel cooperative interference cancellation strategy was proposed in [6], by utilizing the existing backhaul links between the cellular GBSs. Moreover, the non-orthogonal multiple access (NOMA) technique was exploited in [7], where a properly selected subset of the GBSs firstly

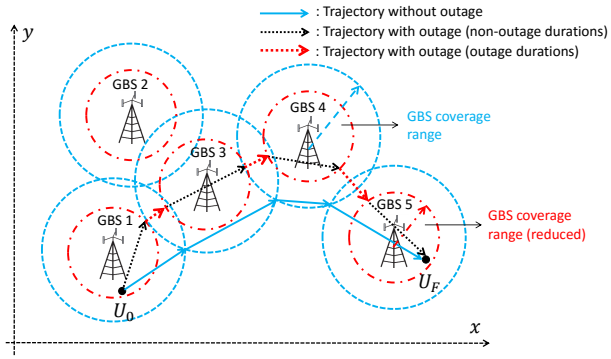

Fig. 1. Illustration of trajectories without versus with communication outage.

decode the UAV's signals, and then cancel them to decode the signals from the terrestrial users.

Furthermore, note that different from the terrestrial users who are typically static or move randomly, UAVs possess flexible and controllable mobility in the three-dimensional (3D) space, which can be exploited to enhance the communication performances with GBSs by proactively creating favorable channel conditions via *trajectory design*. For example, the UAV's trajectory in a mission can be designed to shorten the distances with their associated GBSs along its flight and thus achieve reduced path loss for communication. This promising new approach has been recently investigated in [1], [11]. Specifically, our prior work [1] first studied the trajectory design for a cellular-connected UAV in the mission of flying from an initial location to a final location, while communicating with its associated GBSs during the flight under a prescribed quality-of-service (QoS) requirement in terms of minimum signal-to-noise ratio (SNR) for decoding at the receiver, which needs to be satisfied at all time. Under this stringent constraint, the UAV trajectory was optimized in [1] to minimize the UAV's mission completion time.

However, in practice, due to various considerations such as GBSs' locations and coverage range, as well as UAV's trajectory and mobility constraints, a constant SNR target may not be met at certain time periods during the UAV's flight, each of which is termed as an *outage duration*. For example, in Fig. 1, we compare the two cases where there is no communication outage along the UAV trajectory (the setup considered in [1]) versus that when there are outage durations due to the increased SNR target which results in reduced coverage range of each GBS.

In this paper, we extend our work in [1] to a more general as well as challenging scenario where outage durations are inevitable in the UAV's flight, as also considered in [11]. Our main contributions are summarized as follows.

- First, we propose a general *outage cost function* to characterize the communication outage performance during the UAV's flight, which is non-decreasing with the outage durations. It

is shown that the proposed cost function includes the total outage duration and the maximum outage duration as two special cases, which are usually of high practical interest in UAV communications.

- Next, based on the proposed outage cost function, we formulate a UAV trajectory optimization problem to minimize its mission completion time from given initial to final locations, subject to a new constraint on the maximum tolerable outage cost over its flight. Note that for the special case of zero outage cost constraint, this problem reduces to that considered in [1]. However, for the general case with non-zero outage cost incurred, the problem is more involved and thus more challenging to solve as compared to that considered in [1]. As a result, the solution in [1] cannot be directly applied to solve our new problem in this paper under the general setup.
- To tackle this new problem, we first transform it to an equivalent problem in a more tractable form, by examining the sequence of GBS-UAV associations along the trajectory. Based on the new formulation, the optimal trajectory is shown to consist of connected line segments only, which further reduces the problem to a joint optimization of the *GBS-UAV association sequence* and a set of *waypoint locations* that specify the trajectory line segments. Although the obtained problem is still non-convex, we first propose a low-complexity graph based algorithm to check its feasibility efficiently. Then, by further exploring the problem structure, we propose a method based on graph theory and convex optimization to obtain its optimal solution. Moreover, by applying appropriate bounding and approximation techniques, we propose a more efficient method to find a suboptimal solution with polynomial complexity by using the *Lagrange relaxation method* and *shortest path algorithms* in graph theory. Furthermore, we investigate the problem for the special case taking the maximum outage duration as the cost function, and for this case propose new algorithms of even lower complexity for checking the problem feasibility and finding both optimal and high-quality suboptimal solutions.
- Finally, the performance and complexity of the proposed trajectory designs are evaluated via numerical examples. It is worth noting that the problem considered in this paper for the special case with the maximum outage duration as the cost function has been studied in [11], where a dynamic programming (DP) based method was proposed to find an approximate solution in general. It is shown in this paper that our proposed trajectory designs outperform the DP-based solution in terms of both performance and complexity, thanks to the joint

exploitation of graph theory and convex optimization in our proposed designs. In addition, it is shown that the trajectory design is critically dependent on the outage cost constraint as well as the SNR target.

The remainder of this paper is organized as follows. Section II presents the system model. Section III presents the problem formulation. Section IV presents an equivalent reformulation of the problem as well as the optimal solution structure. For the reformulated problem, Section V proposes an efficient approach to check its feasibility, and Section VI presents both the optimal and suboptimal solutions. Section VII presents the alternative solutions for the special case of maximum outage duration as the cost function. Numerical examples are provided in Section VIII. Finally, Section IX concludes the paper.

Notations: Scalars and vectors are denoted by lower-case letters and boldface lower-case letters, respectively. $\boldsymbol{z}^T$ and $\|\boldsymbol{z}\|$ denote the transpose and the Euclidean norm of a vector $\boldsymbol{z}$, respectively. $|\mathcal{X}|$ denotes the cardinality of a set $\mathcal{X}$. $\mathcal{X} \cup \mathcal{Y}$ denotes the union of two sets $\mathcal{X}$ and $\mathcal{Y}$. $\mathcal{O}(\cdot)$ denotes the standard big-O notation. $\mathbb{R}^{m\times n}$ denotes the space of $m \times n$ real matrices. $\mathbb{C}$ denotes the space of complex numbers. The distribution of a circularly symmetric complex Gaussian (CSCG) random variable with mean μ and variance σ^2 is denoted by $\mathcal{CN}(\mu, \sigma^2)$; and $\sim$ stands for "distributed as". For a time-dependent function $\boldsymbol{x}(t)$, $\dot{\boldsymbol{x}}(t)$ denotes its first-order derivative with respect to time t.

II. System Model

Consider a cellular-connected UAV and $M \geq 1$ GBSs that may potentially be associated with the UAV during its flight mission. We assume that the UAV flies at a constant altitude of H meters (m), and all the M GBSs have the same height of $H_{\rm G}$ m, with $H_{\rm G} \ll H$. The mission of the UAV is to fly from an initial location U_0 to a final location U_F, while communicating with the cellular network. By considering a 3D Cartesian coordinate system, we denote (x_0, y_0, H) and (x_F, y_F, H) as the coordinates of U_0 and U_F, respectively; $(a_m, b_m, H_{\rm G})$ as the coordinate of each mth GBS; and $(x(t), y(t), H),\ 0 \leq t \leq T$ as the time-varying coordinate of the UAV, with T denoting the mission completion time. For ease of exposition, we further define $\boldsymbol{u}_0 = [x_0, y_0]^T$, $\boldsymbol{u}_F = [x_F, y_F]^T$, $\boldsymbol{g}_m = [a_m, b_m]^T$, and $\boldsymbol{u}(t) = [x(t), y(t)]^T$ to represent the above coordinates projected on the horizontal plane, respectively, where $\boldsymbol{u}(0) = \boldsymbol{u}_0$ and $\boldsymbol{u}(T) = \boldsymbol{u}_F$.

In this paper, we assume that the channel between the UAV and each GBS is dominated by the LoS link. We also consider that the UAV is equipped with one single antenna, while each

GBS is equipped with multiple antennas that have a fixed directional gain towards the UAV and hence can be equivalently treated as a single antenna for simplicity. Note that at each time instant t, the distance between the mth GBS and the UAV is given by

$$d_m(t) = \sqrt{(H - H_{\mathrm{G}})^2 + \|\boldsymbol{u}(t) - \boldsymbol{g}_m\|^2}, \quad m \in \mathcal{M}, \tag{1}$$

where $\mathcal{M} = \{1, ..., M\}$ denotes the GBS index set. Therefore, the channel coefficient between the mth GBS and the UAV at time t is expressed as

$$h_m(t) = \sqrt{\beta_0 / d_m^2(t)} e^{-j\frac{2\pi}{\lambda} d_m(t)}, \quad m \in \mathcal{M}, \tag{2}$$

where β_0 denotes the channel power gain at the reference distance of $d_0 = 1$ m, and λ denotes the wavelength in m [12]. We assume that the UAV is associated with one GBS indexed by $I(t) \in \mathcal{M}$ at each time instant t during its mission. For convenience, we consider the scenario of downlink communication from each GBS to the UAV, while the results of this paper are also applicable to the uplink communication. The received signal at the UAV at one particular symbol interval can be expressed as

$$y = \sqrt{P} h_{I(t)}(t) s + z, \quad 0 \le t \le T, \tag{3}$$

where P denotes the transmission power at associated GBS $I(t)$; s denotes the information symbol sent by GBS $I(t)$, which is assumed to be a random variable with zero mean and unit variance; and $z \sim \mathcal{CN}(0, \sigma^2)$ denotes the CSCG noise with zero mean and variance σ^2. For simplicity, we assume that a dedicated time-frequency channel is assigned to the UAV communication, and hence there is no interference from other non-associated GBSs. According to (2), the GBS that is *closest to* the UAV at each time instant t yields the maximum channel power gain with the UAV, thus should be associated with the UAV for communication, i.e., $I(t) = \arg\min_{m \in \mathcal{M}} \|\boldsymbol{u}(t) - \boldsymbol{g}_m\|$. Consequently, the SNR at the UAV receiver at each time instant t is given by

$$\rho(t) = \frac{\gamma_0}{(H - H_{\mathrm{G}})^2 + \min\limits_{m \in \mathcal{M}} \|\boldsymbol{u}(t) - \boldsymbol{g}_m\|^2}, \quad 0 \le t \le T, \tag{4}$$

where $\gamma_0 = \frac{P\beta_0}{\sigma^2}$ denotes the reference SNR at $d_0 = 1$ m.

We consider delay-limited communications between the GBS and UAV for e.g., exchanging time-critical C&C messages, real-time video streaming, and so on. In practice, this type of communications generally requires a minimum SNR target to be satisfied at the receiver to meet

the prescribed QoS requirements, namely $\rho(t) \geq \bar{\rho}$, where $\bar{\rho}$ denotes the SNR target. It can be shown from (4) that this requirement is equivalent to the following constraint on the horizontal distance between the UAV and its associated (closest) GBS at each time instant t:

$$\min_{m \in \mathcal{M}} \|\boldsymbol{u}(t) - \boldsymbol{g}_m\| \leq \bar{d}, \tag{5}$$

where $\bar{d} \triangleq \sqrt{\frac{\gamma_0}{\bar{\rho}} - (H - H_{\mathrm{G}})^2}$. Clearly, it is desirable to design the UAV trajectory $\{\boldsymbol{u}(t), 0 \leq t \leq T\}$ such that (5) is satisfied for all time instants $t \in [0, T]$ throughout its mission, as pursued in our previous work [1]. However, as discussed in Section I, this may not be always feasible in practice, since the existence of such trajectory depends on various factors such as the required communication range $\bar{d}$, the number of GBSs and their locations, etc. For any given UAV trajectory, an *outage* event for UAV communication occurs at time t if (5) is not satisfied.

Motivated by the above practical issue in UAV trajectory design, we consider a new performance metric for delay-sensitive UAV communications, which captures the outage events during the UAV flight. Specifically, for each time instant t during the UAV mission, denote $t_{\mathrm{N}}(t)$, $t_{\mathrm{N}}(t) \leq t$, as the latest time instant at which there is no outage, i.e.,

$$t_{\mathrm{N}}(t) = \max\left\{\hat{t} \in [0, t] : \min_{m \in \mathcal{M}} \|\boldsymbol{u}(\hat{t}) - \boldsymbol{g}_m\| \leq \bar{d}\right\}, \quad 0 \leq t \leq T. \tag{6}$$

Note that $t_{\mathrm{N}}(t) = t$ if there is no outage at time t, while $t_{\mathrm{N}}(t) < t$ represents that outage occurs from $t_{\mathrm{N}}(t)$ to t for a finite duration of $t - t_{\mathrm{N}}(t)$. Thus, the duration that the UAV has remained in outage, or the "*current outage duration*", at time instant t is given by

$$O_{\mathrm{D}}(t) = t - t_{\mathrm{N}}(t), \quad 0 \leq t \leq T. \tag{7}$$

Note that outage duration is a critical performance indicator in delay-sensitive communications. For example, if the C&C messages from the GBSs cannot be sent to the UAV reliably (i.e., when outage occurs) for a sufficiently long period, then the UAV may be "out of control"; as another example, if the real-time video streaming service is interrupted for too long, the user experience will degrade significantly. Furthermore, with its time-varying location along the trajectory, the UAV may experience multiple outage durations in its flight, all of which need to be taken into consideration. To characterize the overall effect of the outage events/durations over the UAV's flight to the communication performance, we propose the following *outage cost function*:

$$f_{\mathrm{O},\alpha} \triangleq \left(\int_0^T O_{\mathrm{D}}(t)^{\alpha} dt\right)^{\frac{1}{\alpha+1}} = \left(\int_0^T (t - t_{\mathrm{N}}(t))^{\alpha} dt\right)^{\frac{1}{\alpha+1}}, \tag{8}$$

where $\alpha \geq 0$ is an adjustable parameter. Note that there are two important properties of the proposed outage cost function $f_{\mathrm{O},\alpha}$. First, $f_{\mathrm{O},\alpha}$ generally increases as the outage duration at each tth time instant, $O_{\mathrm{D}}(t)$, increases, since this leads to degraded outage performance; while $f_{\mathrm{O},\alpha} = 0$ if and only if there is no outage in the UAV's entire flight. Second, $f_{\mathrm{O},\alpha}$ can be regarded as the "generalized" mean of the outage durations at all time during the UAV's flight, which is more dominated by the time instants with large $O_{\mathrm{D}}(t)$ as α increases. In practice, the value of α can be set flexibly to cater for different UAV applications by imposing different "weights" to different outage durations. In the following, we take three examples of α, namely, $\alpha = 0$, $\alpha = 1$, and $\alpha \to \infty$, to discuss their corresponding outage cost functions of high practical interest, respectively.

1) $\alpha = 0$ *(total outage duration)*: In this case, we have

$$f_{\mathrm{O},0} = \int_0^T (t - t_{\mathrm{N}}(t))^0 dt = \int_0^T O(t) dt, \tag{9}$$

where $O(t)$ represents the outage event indicator function, with $O(t) = 0$ if $t = t_{\mathrm{N}}(t)$, i.e., there is no outage at time t, and $O(t) = 1$ if $t > t_{\mathrm{N}}(t)$.[1] Note that $f_{\mathrm{O},0}$ in (9) represents the total outage duration of the UAV in its flight, which satisfies $f_{\mathrm{O},0} \in [0, T]$.

2) $\alpha = 1$ *(square root of total age-of-information)*: In this case, we have

$$f_{\mathrm{O},1} = \sqrt{\int_0^T (t - t_{\mathrm{N}}(t)) dt}. \tag{10}$$

Note that for each time instant t, the outage duration $O_{\mathrm{D}}(t) = t - t_{\mathrm{N}}(t)$ is actually the time elapsed since the "freshest" information transmission with satisfactory QoS, which is also termed as the *"age-of-information"* [13]. Thus, $f_{\mathrm{O},1}$ in (10) represents the square root of the total age-of-information throughout the UAV mission, which can be shown to satisfy $f_{\mathrm{O},1} \in \left[0, \frac{\sqrt{2}}{2} T\right]$.

3) $\alpha \to \infty$ *(maximum outage duration)*: In this case, we have

$$f_{\mathrm{O},\infty} = \lim_{\alpha \to \infty} f_{\mathrm{O},\alpha} = \lim_{\alpha \to \infty} \left(\frac{1}{T} \int_0^T (t - t_{\mathrm{N}}(t))^\alpha dt \right)^{\frac{1}{\alpha}} \overset{(a)}{=} \max_{0 \leq t \leq T} t - t_{\mathrm{N}}(t), \tag{11}$$

where (a) can be derived based on properties of the generalized mean. Note that $f_{\mathrm{O},\infty} = \max\limits_{0 \leq t \leq T} O_{\mathrm{D}}(t)$ represents the maximum outage duration during the UAV's flight, which satisfies $f_{\mathrm{O},\infty} \in [0, T]$.

[1]Without loss of generality, we assume that $0^\alpha = 0$ holds for any $\alpha \in [0, \infty)$ in this paper.

In practice, the outage cost function $f_{\mathrm{O},\alpha}$ usually needs to be designed below a certain value for delay-sensitive communications, e.g., to ensure that the maximum outage duration is no larger than a tolerable threshold for the case of $\alpha \to \infty$. Therefore, it is critical to design the UAV trajectory $\{\boldsymbol{u}(t), 0 \le t \le T\}$ such that a maximum outage cost constraint specified by $\bar{f}_{\mathrm{O},\alpha}$ can be satisfied, i.e., $f_{\mathrm{O},\alpha} \le \bar{f}_{\mathrm{O},\alpha}$, as investigated in the sequel of this paper.

III. Problem Formulation

In this paper, we aim to minimize the UAV's mission completion time T by optimizing the UAV trajectory $\{\boldsymbol{u}(t), 0 \le t \le T\}$, subject to the UAV's initial and final location constraints, as well as the outage cost constraint $f_{\mathrm{O},\alpha} \le \bar{f}_{\mathrm{O},\alpha}$, where the values of α and $\bar{f}_{\mathrm{O},\alpha}$ are pre-determined based on the specific application. We assume that the UAV flies at its maximum speed $V_{\max}$ (in m/s) during its mission, namely, $\|\dot{\boldsymbol{u}}(t)\| = V_{\max}$, where $\dot{\boldsymbol{u}}(t)$ denotes the UAV velocity.[2] Therefore, we formulate the following optimization problem:

$$\text{(P1)} \quad \min_{T,\{\boldsymbol{u}(t),0\le t\le T\}} \quad T \tag{12}$$

$$\text{s.t.} \quad \boldsymbol{u}(0) = \boldsymbol{u}_0 \tag{13}$$

$$\boldsymbol{u}(T) = \boldsymbol{u}_F \tag{14}$$

$$\left(\int_0^T (t - t_{\mathrm{N}}(t))^{\alpha} dt\right)^{\frac{1}{\alpha+1}} \le \bar{f}_{\mathrm{O},\alpha} \tag{15}$$

$$\|\dot{\boldsymbol{u}}(t)\| = V_{\max}, \quad 0 \le t \le T. \tag{16}$$

It is worth noting that for the special case with $\bar{f}_{\mathrm{O},\alpha} = 0$, i.e., no outage is allowed during the UAV mission, (P1) is equivalent to that studied in our prior work [1]. Thus, in this paper, we focus on the case of (P1) with $\bar{f}_{\mathrm{O},\alpha} > 0$, i.e., there are non-zero outage durations during the UAV's flight.

Note that (P1) is a non-convex optimization problem, and there are no standard methods to obtain its optimal solution efficiently. Moreover, even checking the feasibility of (P1) for a given $\bar{f}_{\mathrm{O},\alpha} > 0$ is a non-trivial problem. To tackle these difficulties, in the following, we first reformulate (P1) into a more tractable form, based on which we then propose efficient algorithms to check its feasibility and obtain its optimal as well as high-quality suboptimal solutions.

[2]It can be easily shown that letting the UAV fly at its maximum speed is optimal for our considered problem, which is thus assumed in this paper.

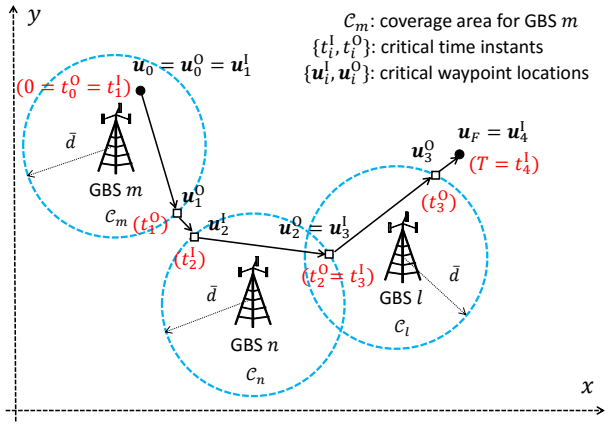

Fig. 2. Illustration of GBS-UAV associations with $\boldsymbol{I} = [m, n, l]^T$.

IV. Problem Reformulation and Optimal Solution Structure

In this section, we transform (P1) to an equivalent problem in a more tractable form. First, note that one major difficulty in solving (P1) lies in the complicated expression of $t_{\mathrm{N}}(t)$ given in (6). To tackle this difficulty, we express $t_{\mathrm{N}}(t)$ as well as its associated constraint (15) in simplified forms by introducing a so-called *GBS-UAV association sequence*, which specifies a set of GBSs that are successively associated with the UAV to achieve non-outage communications. Then, we show that the optimal trajectory of the UAV should follow a path constituting *connected line segments*, based on which (P1) can be simplified to jointly design the GBS-UAV association sequence and the corresponding set of *waypoint locations* that specify all line segments in the UAV trajectory.

A. GBS-UAV Association Sequence and Problem Reformulation

First, for ease of exposition, we define a so-called *coverage area* for each GBS m as

$$\mathcal{C}_m = \left\{ \boldsymbol{u} \in \mathbb{R}^{2\times 1} : \|\boldsymbol{u} - \boldsymbol{g}_m\| \leq \bar{d} \right\}, \quad m \in \mathcal{M}, \tag{17}$$

which is a disk region on the horizontal plane centered at GBS m's location $\boldsymbol{g}_m$ with radius $\bar{d}$, as illustrated in Fig. 2. With (17), we say that at each time instant t, the UAV is *covered by* GBS m, i.e., it can be served by GBS m without outage, if its horizontal location lies in $\mathcal{C}_m$, i.e., $\boldsymbol{u}(t) \in \mathcal{C}_m$. On the other hand, an outage event occurs if the UAV is not covered by any GBS, i.e., $\boldsymbol{u}(t) \notin \cup_{m\in\mathcal{M}} \mathcal{C}_m$.

Next, we introduce an auxiliary vector $\boldsymbol{I} = [I_1, ..., I_N]^T$ with $I_i \in \mathcal{M}, \ \forall i \in \{1, ..., N\}$, as the *GBS-UAV association sequence*, which consists of the indices of GBSs that successively serve the UAV to achieve non-outage communications. Moreover, we introduce a set of auxiliary

variables $\{t_i^{\rm I}, t_i^{\rm O}\}_{i=1}^N$ as the *critical time instants*, where $t_i^{\rm I}$ and $t_i^{\rm O}$ denote the time instants that the UAV starts to be covered by GBS I_i and stops being covered by it, respectively, with $0 \le t_1^{\rm I} \le t_1^{\rm O} \le t_2^{\rm I} \le ... \le t_N^{\rm O} \le T$. Correspondingly, the UAV is first covered by GBS I_1 from $t_1^{\rm I}$ to $t_1^{\rm O}$, then by GBS I_2 from $t_2^{\rm I}$ to $t_2^{\rm O}$, etc., and finally covered by GBS I_N from $t_N^{\rm I}$ to $t_N^{\rm O}$. Note that for any $i \in \{2, ..., N\}$, if $t_{i-1}^{\rm O} = t_i^{\rm I}$ holds, then the UAV is seamlessly handed over from GBS I_{i-1} to GBS I_i without any outage; otherwise, outage occurs during the handover from $t_{i-1}^{\rm O}$ to $t_i^{\rm I}$. For convenience, we further define $t_0^{\rm O} \triangleq 0$ and $t_{N+1}^{\rm I} \triangleq T$. In Fig. 2, we illustrate $\{t_i^{\rm I}, t_i^{\rm O}\}_{i=1}^N$ and $t_0^{\rm O}$, $t_{N+1}^{\rm I}$ by taking the example of $\boldsymbol{I} = [m, n, l]^T$.

With the above definitions, $t_{\rm N}(t)$ in (6) can be rewritten as

$$t_{\rm N}(t) = \begin{cases} t, & t \in [t_i^{\rm I}, t_i^{\rm O}), \quad i \in \{1, ..., N\} \\ t_{i-1}^{\rm O}, & t \in [t_{i-1}^{\rm O}, t_i^{\rm I}), \ i \in \{1, ..., N+1\}. \end{cases} \tag{18}$$

The outage cost function $f_{{\rm O},\alpha}$ in (8) is thus rewritten as

$$f_{{\rm O},\alpha} = \left(\sum_{i=1}^{N+1} \int_{t_{i-1}^{\rm O}}^{t_i^{\rm I}} (t - t_{i-1}^{\rm O})^\alpha dt \right)^{\frac{1}{\alpha+1}} = \left(\sum_{i=1}^{N+1} \frac{(t_i^{\rm I} - t_{i-1}^{\rm O})^{\alpha+1}}{\alpha+1} \right)^{\frac{1}{\alpha+1}}. \tag{19}$$

Then, we are ready to present the following proposition.

Proposition 1: (P1) is equivalent to the following problem:

$$\text{(P2)} \quad \min_{\substack{T, \{\boldsymbol{u}(t), 0 \le t \le T\} \\ \boldsymbol{I}, \{t_i^{\rm I}, t_i^{\rm O}\}_{i=1}^N}} \quad T \tag{20}$$

$$\text{s.t.} \quad (13), (14), (16) \tag{21}$$

$$\|\boldsymbol{u}(t) - \boldsymbol{g}_{I_i}\| \le \bar{d}, \quad t_i^{\rm I} \le t \le t_i^{\rm O}, \quad i = 1, ..., N \tag{22}$$

$$t_0^{\rm O} = 0 \tag{23}$$

$$t_{N+1}^{\rm I} = T \tag{24}$$

$$t_{i-1}^{\rm O} \le t_i^{\rm I} \le t_i^{\rm O} \le T, \quad i = 1, ..., N \tag{25}$$

$$I_i \in \mathcal{M}, \quad i = 1, ..., N \tag{26}$$

$$\left(\sum_{i=1}^{N+1} \frac{(t_i^{\rm I} - t_{i-1}^{\rm O})^{\alpha+1}}{\alpha+1} \right)^{\frac{1}{\alpha+1}} \le \bar{f}_{{\rm O},\alpha}. \tag{27}$$

Proof: Please refer to Appendix A. ■

Denote the horizontal location of the UAV at the critical time instants $t_i^{\rm I}$ and $t_i^{\rm O}$ as $\boldsymbol{u}_i^{\rm I} \triangleq \boldsymbol{u}(t_i^{\rm I})$ and $\boldsymbol{u}_i^{\rm O} \triangleq \boldsymbol{u}(t_i^{\rm O})$, respectively. Note that since the UAV is covered by GBS I_i at both $t_i^{\rm I}$ and $t_i^{\rm O}$, we have $\boldsymbol{u}_i^{\rm I} \in \mathcal{C}_{I_i}$, $\boldsymbol{u}_i^{\rm O} \in \mathcal{C}_{I_i}$, $i = 1, ..., N$. In the following, we refer to $\{\boldsymbol{u}_i^{\rm I}, \boldsymbol{u}_i^{\rm O}\}_{i=1}^N$ as the set

of *critical waypoint locations*, as also illustrated in Fig. 2 for the example of $\boldsymbol{I} = [m, n, l]^T$. In addition, note that we also have $\boldsymbol{u}_0^{\mathrm{O}} \triangleq \boldsymbol{u}_0$ and $\boldsymbol{u}_{N+1}^{\mathrm{I}} \triangleq \boldsymbol{u}_F$ by definition.

B. Structure of Optimal UAV Trajectory

Based on the reformulated problem (P2), we show a simplified structure of the optimal UAV trajectory in the following proposition.

Proposition 2 (Trajectory with Connected Line Segments): The optimal solution to (P2) satisfies the following conditions:

$$t_i^{\mathrm{I}} = t_{i-1}^{\mathrm{O}} + \frac{\|\boldsymbol{u}_i^{\mathrm{I}} - \boldsymbol{u}_{i-1}^{\mathrm{O}}\|}{V_{\max}}, \quad i = 1, ..., N+1, \tag{28}$$

$$t_i^{\mathrm{O}} = t_i^{\mathrm{I}} + \frac{\|\boldsymbol{u}_i^{\mathrm{O}} - \boldsymbol{u}_i^{\mathrm{I}}\|}{V_{\max}}, \quad i = 1, ..., N, \tag{29}$$

$$\boldsymbol{u}(t) = \begin{cases} \boldsymbol{u}_{i-1}^{\mathrm{O}} + (t - t_{i-1}^{\mathrm{O}}) V_{\max} \frac{\boldsymbol{u}_i^{\mathrm{I}} - \boldsymbol{u}_{i-1}^{\mathrm{O}}}{\|\boldsymbol{u}_i^{\mathrm{I}} - \boldsymbol{u}_{i-1}^{\mathrm{O}}\|}, & t \in [t_{i-1}^{\mathrm{O}}, t_i^{\mathrm{I}}], \ i = 1, ..., N+1 \\ \boldsymbol{u}_i^{\mathrm{I}} + (t - t_i^{\mathrm{I}}) V_{\max} \frac{\boldsymbol{u}_i^{\mathrm{O}} - \boldsymbol{u}_i^{\mathrm{I}}}{\|\boldsymbol{u}_i^{\mathrm{O}} - \boldsymbol{u}_i^{\mathrm{I}}\|}, & t \in [t_i^{\mathrm{I}}, t_i^{\mathrm{O}}], \quad i = 1, ..., N, \end{cases} \tag{30}$$

$$T = \sum_{i=1}^{N+1} \frac{\|\boldsymbol{u}_i^{\mathrm{I}} - \boldsymbol{u}_{i-1}^{\mathrm{O}}\|}{V_{\max}} + \sum_{i=1}^{N} \frac{\|\boldsymbol{u}_i^{\mathrm{O}} - \boldsymbol{u}_i^{\mathrm{I}}\|}{V_{\max}}. \tag{31}$$

Proof: Please refer to Appendix B. ■

Note that according to (28)–(31), the UAV should fly from U_0 to U_F following a path consisting of *connected line segments* only, where the end points that determine these connected line segments are the critical waypoints with horizontal locations $\{\boldsymbol{u}_0, \boldsymbol{u}_1^{\mathrm{I}}, \boldsymbol{u}_1^{\mathrm{O}}, \boldsymbol{u}_2^{\mathrm{I}}, \boldsymbol{u}_2^{\mathrm{O}}, ..., \boldsymbol{u}_N^{\mathrm{I}}, \boldsymbol{u}_N^{\mathrm{O}}, \boldsymbol{u}_F\}$. Following this optimal trajectory structure, the outage cost function $f_{\mathrm{O},\alpha}$ in (19) can be equivalently rewritten as $f_{\mathrm{O},\alpha} = \frac{\left(\sum_{i=1}^{N+1} \|\boldsymbol{u}_i^{\mathrm{I}} - \boldsymbol{u}_{i-1}^{\mathrm{O}}\|^{\alpha+1}\right)^{\frac{1}{\alpha+1}}}{V_{\max}(\alpha+1)^{\frac{1}{\alpha+1}}}$. Hence, it can be shown that (P2) is equivalent to the following problem based on Proposition 2:

$$\text{(P3)} \quad \min_{\boldsymbol{I}, \{\boldsymbol{u}_i^{\mathrm{I}}, \boldsymbol{u}_i^{\mathrm{O}}\}_{i=1}^N} \quad \sum_{i=1}^{N+1} \|\boldsymbol{u}_i^{\mathrm{I}} - \boldsymbol{u}_{i-1}^{\mathrm{O}}\| + \sum_{i=1}^{N} \|\boldsymbol{u}_i^{\mathrm{O}} - \boldsymbol{u}_i^{\mathrm{I}}\| \tag{32}$$

$$\text{s.t.} \quad \boldsymbol{u}_0^{\mathrm{O}} = \boldsymbol{u}_0 \tag{33}$$

$$\boldsymbol{u}_{N+1}^{\mathrm{I}} = \boldsymbol{u}_F \tag{34}$$

$$\|\boldsymbol{u}_i^{\mathrm{I}} - \boldsymbol{g}_{I_i}\| \le \bar{d}, \quad i = 1, ..., N \tag{35}$$

$$\|\boldsymbol{u}_i^{\mathrm{O}} - \boldsymbol{g}_{I_i}\| \le \bar{d}, \quad i = 1, ..., N \tag{36}$$

$$I_i \in \mathcal{M}, \quad i = 1, ..., N \tag{37}$$

$$\frac{\left(\sum_{i=1}^{N+1} \|\boldsymbol{u}_i^{\mathrm{I}} - \boldsymbol{u}_{i-1}^{\mathrm{O}}\|^{\alpha+1}\right)^{\frac{1}{\alpha+1}}}{V_{\max}(\alpha+1)^{\frac{1}{\alpha+1}}} \le \bar{f}_{\mathrm{O},\alpha}. \tag{38}$$

Notice that Problem (P3) is a joint optimization problem for the GBS-UAV association sequence $\boldsymbol{I}$ and the corresponding waypoint locations $\{\boldsymbol{u}_i^{\mathrm{I}}, \boldsymbol{u}_i^{\mathrm{O}}\}_{i=1}^N$. Furthermore, (P3) is equivalent to (P1), but (P3) involves a significantly less number of variables as compared to (P1), thanks to the optimal line-segment structure of the UAV trajectory. Note that (P1) is feasible if and only if (P3) is feasible, thus the feasibility of (P1) can be equivalently verified by checking the feasibility of (P3); moreover, the optimal solution to (P1) can be obtained by substituting the optimal solution obtained for (P3) into (28)–(31). Therefore, we focus on solving (P3) in the next.

Last, we provide the following proposition, which helps to significantly reduce the potentially optimal set of $\boldsymbol{I}$ for (P3).

Proposition 3 (Non-Repeated GBS-UAV Association): Without loss of optimality to Problem (P3), the GBS-UAV association sequence $\boldsymbol{I}$ can be assumed to satisfy:

$$I_i \neq I_j, \quad \forall i \neq j,\ i,j = 1, ..., N. \tag{39}$$

Proof: Please refer to Appendix C. ■

With Proposition 3, the potentially optimal set for $\boldsymbol{I}$ can be characterized by the constraints in (37) and (39), and (P3) is equivalent to itself with the additional constraints in (39). In the following, we consider (P3) with the constraints in (39).

V. Feasibility Check

Prior to solving Problem (P3), we check its feasibility in this section. Note that (P3) is feasible if and only if the problem below is feasible, and its optimal value is no larger than $\bar{f}_{\mathrm{O},\alpha}$:

$$\text{(P3-F)} \quad \min_{\boldsymbol{I}, \{\boldsymbol{u}_i^{\mathrm{I}}, \boldsymbol{u}_i^{\mathrm{O}}\}_{i=1}^N} \quad \frac{\left(\sum_{i=1}^{N+1} \|\boldsymbol{u}_i^{\mathrm{I}} - \boldsymbol{u}_{i-1}^{\mathrm{O}}\|^{\alpha+1}\right)^{\frac{1}{\alpha+1}}}{V_{\max}(\alpha+1)^{\frac{1}{\alpha+1}}} \tag{40}$$

$$\text{s.t.} \quad (33), (34), (35), (36), (37), (39). \tag{41}$$

It is worth noting that the optimal value of (P3-F) represents the minimum achievable outage cost of the UAV's flight. For (P3-F), we have the following proposition.[3]

[3]For ease of exposition and without loss of generality, we assume that $\|\boldsymbol{u}_F - \boldsymbol{u}_0\| > V_{\max}\bar{f}_{\mathrm{O},\alpha}(\alpha+1)^{\frac{1}{\alpha+1}}$ holds in the sequel, thus $N = 0$ is not feasible for (P3).

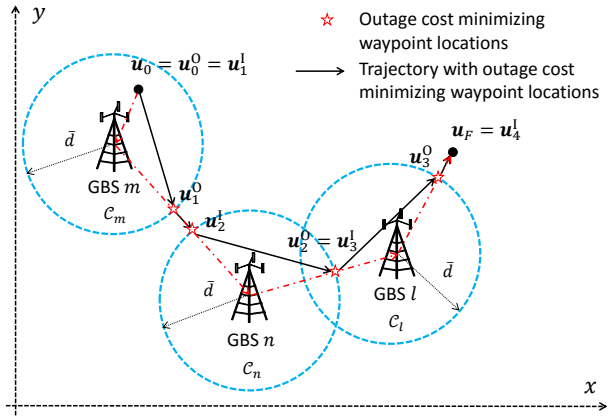

Fig. 3. Illustration of outage cost minimizing waypoint locations with $\boldsymbol{I} = [m, n, l]^T$.

Proposition 4 (Outage Cost Minimizing Waypoint Locations): Given any $\boldsymbol{I}$ that satisfies the constraints in (37) and (39), the outage cost function $f_{\mathrm{O},\alpha}$ is minimized as

$$f^{\star}_{\mathrm{O},\alpha}(\boldsymbol{I}) = \frac{1}{V_{\max}(\alpha+1)^{\frac{1}{\alpha+1}}}\Big(\big(\max\{\|\boldsymbol{u}_0 - \boldsymbol{g}_{I_1}\| - \bar{d}, 0\}\big)^{\alpha+1} + \sum_{i=2}^{N} \big(\max\{\|\boldsymbol{g}_{I_i} - \boldsymbol{g}_{I_{i-1}}\| - 2\bar{d}, 0\}\big)^{\alpha+1} + \big(\max\{\|\boldsymbol{u}_F - \boldsymbol{g}_{I_N}\| - \bar{d}, 0\}\big)^{\alpha+1}\Big)^{\frac{1}{\alpha+1}}. \tag{42}$$

An optimal solution of $\{\boldsymbol{u}_i^{\mathrm{I}}, \boldsymbol{u}_i^{\mathrm{O}}\}_{i=1}^N$ to (P3-F) is given by

$$\boldsymbol{u}_1^{\mathrm{I}} = \begin{cases} \boldsymbol{u}_0, & \text{if } \|\boldsymbol{u}_0 - \boldsymbol{g}_{I_1}\| \le \bar{d} \\ \boldsymbol{g}_{I_1} - \bar{d}\frac{\boldsymbol{g}_{I_1} - \boldsymbol{u}_0}{\|\boldsymbol{g}_{I_1} - \boldsymbol{u}_0\|}, & \text{otherwise,} \end{cases} \tag{43}$$

$$\boldsymbol{u}_N^{\mathrm{O}} = \begin{cases} \boldsymbol{u}_F, & \text{if } \|\boldsymbol{u}_F - \boldsymbol{g}_{I_N}\| \le \bar{d} \\ \boldsymbol{g}_{I_N} + \bar{d}\frac{\boldsymbol{u}_F - \boldsymbol{g}_{I_N}}{\|\boldsymbol{u}_F - \boldsymbol{g}_{I_N}\|}, & \text{otherwise,} \end{cases} \tag{44}$$

$$\boldsymbol{u}_{i-1}^{\mathrm{O}} = \boldsymbol{g}_{I_{i-1}} + \bar{d}\frac{\boldsymbol{g}_{I_i} - \boldsymbol{g}_{I_{i-1}}}{\|\boldsymbol{g}_{I_i} - \boldsymbol{g}_{I_{i-1}}\|}, \quad i = 2, ..., N, \tag{45}$$

$$\boldsymbol{u}_i^{\mathrm{I}} = \begin{cases} \boldsymbol{u}_{i-1}^{\mathrm{O}}, & \text{if } \|\boldsymbol{g}_{I_i} - \boldsymbol{g}_{I_{i-1}}\| \le 2\bar{d} \\ \boldsymbol{g}_{I_i} - \bar{d}\frac{\boldsymbol{g}_{I_i} - \boldsymbol{g}_{I_{i-1}}}{\|\boldsymbol{g}_{I_i} - \boldsymbol{g}_{I_{i-1}}\|}, & \text{otherwise,} \end{cases} \quad i = 2, ..., N. \tag{46}$$

Proof: Please refer to Appendix D. ■

Note that Proposition 4 suggests that the outage cost function is minimized by placing the waypoint locations $\boldsymbol{u}_i^{\mathrm{I}}$ and $\boldsymbol{u}_{i-1}^{\mathrm{O}}$ on the boundaries of $\mathcal{C}_{I_i}$ or $\mathcal{C}_{I_{i-1}}$ and at the same time on the connected line segment between GBSs I_{i-1} and I_i, as given in (43)–(46) and illustrated in Fig. 3. In the following, by leveraging Proposition 4, we propose a graph based characterization of (P3-F), based on which the feasibility of (P3) can be checked via evaluating the *shortest path* between

two given vertices in a graph.

Specifically, we construct an undirected weighted graph $G = (V, E)$ [14]. The vertex set V is given by

$$V = \{U_0, G_1, ..., G_M, U_F\}, \tag{47}$$

where U_0 and U_F represent the UAV's initial location and final location, respectively, and each G_m represents the mth GBS. The edge set E is given by

$$E = \{(U_0, G_m) : m \in \mathcal{M}\} \cup \{(G_m, G_n) : m, n \in \mathcal{M}, m \neq n\} \cup \{(U_F, G_m) : m \in \mathcal{M}\}. \tag{48}$$

Moreover, we consider the following set of edge weights for the graph G denoted by W_P's:

$$W_P(U_0, G_m) = \left(\max\{\|\boldsymbol{u}_0 - \boldsymbol{g}_m\| - \bar{d}, 0\}\right)^{\alpha+1}, W_P(U_F, G_m) = \left(\max\{\|\boldsymbol{u}_F - \boldsymbol{g}_m\| - \bar{d}, 0\}\right)^{\alpha+1},$$
$$W_P(G_m, G_n) = \left(\max\{\|\boldsymbol{g}_m - \boldsymbol{g}_n\| - 2\bar{d}, 0\}\right)^{\alpha+1}, \quad m, n \in \mathcal{M}, m \neq n. \tag{49}$$

Note that each $\boldsymbol{I} = [I_1, ..., I_N]^T$ that satisfies the constraints in (37) and (39) in (P3-F) corresponds to a *path* from U_0 to U_F in our constructed graph G denoted by $(U_0, G_{I_1}, ..., G_{I_N}, U_F)$. Furthermore, for each such path specified by $\boldsymbol{I}$, the sum edge weight is given by $s(\boldsymbol{I}) = f^{\star}_{\mathrm{O},\alpha}(\boldsymbol{I})^{\alpha+1} V_{\max}^{\alpha+1}(\alpha+1)$. Thus, the sum edge weight of the *shortest path* from U_0 to U_F in G with respect to weights W_P's is given by $s^{\star} = \min\limits_{I_i \in \mathcal{M}, I_i \neq I_j, i \neq j} s(\boldsymbol{I}) = \min\limits_{I_i \in \mathcal{M}, I_i \neq I_j, i \neq j} f^{\star}_{\mathrm{O},\alpha}(\boldsymbol{I})^{\alpha+1} V_{\max}^{\alpha+1}(\alpha+1)$. Therefore, the optimal value of (P3-F) is given by $f^{\star}_{\mathrm{O},\alpha} = \min\limits_{I_i \in \mathcal{M}, I_i \neq I_j, i \neq j} f^{\star}_{\mathrm{O},\alpha}(\boldsymbol{I}) = \frac{1}{V_{\max}} \left(\frac{s^{\star}}{\alpha+1}\right)^{\frac{1}{\alpha+1}}$, and (P3) is feasible if and only if $f^{\star}_{\mathrm{O},\alpha} \leq \bar{f}_{\mathrm{O},\alpha}$ holds. Note that the shortest path from U_0 to U_F in G can be efficiently obtained via e.g., the Dijkstra algorithm with worst-case complexity $\mathcal{O}(|E| + |V| \log |V|) = \mathcal{O}(M^2)$ [14]. By further noting that constructing the graph G requires a complexity of $\mathcal{O}(M^2)$, the overall complexity for checking the feasibility of (P3) is $\mathcal{O}(M^2)$.

VI. Proposed Solution to (P3)

In this section, we solve Problem (P3) assuming that it has been verified to be feasible. Note that (P3) is a non-convex combinatorial optimization problem due to the discrete variables in $\boldsymbol{I}$, where the length of $\boldsymbol{I}$, N, is also an implicit variable. Moreover, $\boldsymbol{I}$ and $\{\boldsymbol{u}_i^{\mathrm{I}}, \boldsymbol{u}_i^{\mathrm{O}}\}_{i=1}^N$ are coupled by the constraints in (35) and (36), which makes the problem more difficult to solve. In the following, we apply graph theory and convex optimization techniques to overcome the above challenges, and propose the optimal solution as well as a low-complexity suboptimal solution to (P3), respectively.

A. Optimal Solution

Note that with any given GBS-UAV association sequence $\boldsymbol{I}$ that satisfies (37) and (39), (P3) can be equivalently transformed into a convex optimization problem over the waypoint locations $\{\boldsymbol{u}_i^{\mathrm{I}}, \boldsymbol{u}_i^{\mathrm{O}}\}_{i=1}^N$ by replacing the constraint in (38) with $\sum_{i=1}^{N+1} \|\boldsymbol{u}_i^{\mathrm{I}} - \boldsymbol{u}_{i-1}^{\mathrm{O}}\|^{\alpha+1} \leq (\alpha+1)(\bar{f}_{\mathrm{O},\alpha} V_{\max})^{\alpha+1}$, which can be efficiently solved via existing software, e.g., CVX [15], with polynomial complexity over N, e.g., $\mathcal{O}(N^{3.5})$ by casting this problem as a second-order cone program (SOCP) [16]. Moreover, recall that each feasible solution of $\boldsymbol{I}$ to (P3) corresponds to a *path* from U_0 to U_F in graph G constructed in the preceding section, where all such paths can be found via existing algorithms in graph theory, e.g., the depth-first search method with complexity $\mathcal{O}(M!)$ [14]. Hence, the optimal solution to (P3) can be obtained by finding all such paths as well as the corresponding optimal $\{\boldsymbol{u}_i^{\mathrm{I}}, \boldsymbol{u}_i^{\mathrm{O}}\}_{i=1}^N$'s, and selecting the one with the minimum objective value, which requires a worst-case complexity of $\mathcal{O}(M^{3.5}M!)$ since $N \leq M$ holds according to Proposition 3.

B. Suboptimal Solution

To further reduce the complexity of the optimal solution, especially when the number of involved GBSs, M, is practically large (e.g., when the initial and final locations of the UAV, U_0 and U_F, are far apart), we propose an alternative approach for finding an approximate solution to (P3). Specifically, we find an approximate solution of the GBS-UAV association sequence $\boldsymbol{I}$ firstly, and then obtain the optimal waypoint locations $\{\boldsymbol{u}_i^{\mathrm{I}}, \boldsymbol{u}_i^{\mathrm{O}}\}_{i=1}^N$ with the obtained $\boldsymbol{I}$ via CVX (similarly as in the optimal solution). Thus, our remaining task is to find an approximate solution of $\boldsymbol{I}$, for which we present a new *graph* based problem reformulation of (P3) by applying appropriate bounding and approximation techniques, and propose an efficient solution to the formulated problem by applying the *Lagrange relaxation method* and *shortest path* algorithms in graph theory, as shown in the following.

1) Graph based Problem Formulation for Finding Approximate Solution of $\boldsymbol{I}$: Recall from Proposition 4 that (P3) is feasible with given $\boldsymbol{I}$ if and only if the waypoint locations $\{\boldsymbol{u}_i^{\mathrm{I}}, \boldsymbol{u}_i^{\mathrm{O}}\}_{i=1}^N$ given in (43)–(46) satisfy the constraint in (38). Therefore, we can find an approximate solution of $\boldsymbol{I}$ by substituting (43)–(46) into (P3). Nevertheless, note that it is generally difficult to explicitly express the objective function of (P3) with given $\boldsymbol{I}$ and the corresponding waypoints in (43)–(46). Thus, we further consider an upper bound for the objective value of (P3) denoted by s_D, which is given by

$$s_D \le \|\boldsymbol{u}_0 - \boldsymbol{g}_{I_1}\| + \sum_{i=2}^{N} \|\boldsymbol{g}_{I_i} - \boldsymbol{g}_{I_{i-1}}\| + \|\boldsymbol{u}_F - \boldsymbol{g}_{I_N}\| \triangleq \bar{s}_D. \tag{50}$$

Note that (50) can be proved via the triangle inequality and is illustrated in Fig. 3. Hence, to find an approximate solution of $\boldsymbol{I}$, we solve (P3) by replacing its objective function by $\bar{s}_D$ given in (50), and considering the additional constraints in (43)–(46), for which we provide a graph based characterization below. Consider graph $G = (V, E)$ constructed in Section V with one set of edge weights W_P's given in (49). We further consider another set of edge weights for graph G, which is given by

$$\begin{aligned} &W_D(U_0, G_m) = \|\boldsymbol{u}_0 - \boldsymbol{g}_m\|,\ W_D(U_F, G_m) = \|\boldsymbol{u}_F - \boldsymbol{g}_m\|, \\ &W_D(G_m, G_n) = \|\boldsymbol{g}_m - \boldsymbol{g}_n\|, \quad m, n \in \mathcal{M}, m \ne n. \end{aligned} \tag{51}$$

With W_D's, the aforementioned problem can be expressed as

$$\text{(P4)} \quad \min_{\boldsymbol{I} \in \mathcal{I}} \quad W_D(U_0, I_1) + \sum_{i=2}^{N} W_D(I_{i-1}, I_i) + W_D(I_N, U_F) \tag{52}$$

$$\text{s.t.} \quad W_P(U_0, I_1) + \sum_{i=2}^{N} W_P(I_{i-1}, I_i) + W_P(I_N, U_F) \le (\alpha + 1)(\bar{f}_{\mathrm{O},\alpha} V_{\max})^{\alpha+1}, \tag{53}$$

where $\mathcal{I} = \{[I_1, ..., I_N]^T : I_i \in \mathcal{M}, I_i \ne I_j, \forall i \ne j\}$. Note that Problem (P4) is feasible if and only if (P3) is feasible according to the results in Section V. Moreover, (P4) belongs to the class of *constrained shortest path problems* in graph theory, which aims to find a path between two given vertices in a graph (e.g., U_0 to U_F in G) that minimizes the sum edge weight with respect to one set of weights (e.g., W_D's in (P4)), subject to a constraint on the sum edge weight with respect to another set of weights (e.g., W_P's in (P4)). This class of problems has been shown to be NP-hard [17]. Nevertheless, a high-quality approximate solution can be obtained efficiently by applying the *Lagrange relaxation method* [18], [19] together with *shortest path* algorithms in graph theory [14], [20], for which the main idea is introduced next.

2) Proposed Solution to (P4) based on Lagrange Relaxation Method and Shortest Path Algorithms: For ease of exposition, we define $f_D(\boldsymbol{I}) \triangleq W_D(U_0, I_1) + \sum_{i=2}^{N} W_D(I_{i-1}, I_i) + W_D(I_N, U_F)$, and $f_P(\boldsymbol{I}) \triangleq W_P(U_0, I_1) + \sum_{i=2}^{N} W_P(I_{i-1}, I_i) + W_P(I_N, U_F) - (\alpha + 1)(\bar{f}_{\mathrm{O},\alpha} V_{\max})^{\alpha+1}$. The Lagrangian of (P4) is then given by

$$\mathcal{L}(\boldsymbol{I}, \lambda) = f_D(\boldsymbol{I}) + \lambda f_P(\boldsymbol{I}), \tag{54}$$

where λ is the Lagrange multiplier associated with the constraint in (53). The Lagrange dual function is then defined as

$$g(\lambda) = \min_{\boldsymbol{I}\in\mathcal{I}} \mathcal{L}(\boldsymbol{I},\lambda) = \min_{\boldsymbol{I}\in\mathcal{I}} f_D(\boldsymbol{I}) + \lambda f_P(\boldsymbol{I}). \tag{55}$$

With $\lambda \geq 0$, we have $g(\lambda) \leq \bar{s}_D^\star$, where $\bar{s}_D^\star$ denotes the optimal value of (P4). The dual problem of (P4) is then defined as

$$\text{(P4-Dual)} \quad \max_{\lambda\geq 0} \min_{\boldsymbol{I}\in\mathcal{I}} f_D(\boldsymbol{I}) + \lambda f_P(\boldsymbol{I}). \tag{56}$$

Note that (P4-Dual) is a convex optimization problem, whose optimal solution and optimal value denoted by $\lambda^\star$ and $d^\star$, respectively, can be obtained via conventional subgradient-based methods [21]. However, as (P4) is not a convex optimization problem, the duality gap between the dual and primal optimal values $d^\star$ and $\bar{s}_D^\star$ is generally non-zero. As a result, there is no standard method to find even a feasible primal solution based on the optimal dual solution efficiently. In the following, we solve (P4-Dual) via an advanced subgradient-based method introduced in [18], [19], where a feasible solution to (P4) can be obtained in the meanwhile by exploiting the problem structure.

To start with, it can be shown that a solution $\lambda^\star$ is optimal for (P4-Dual) if and only if there exist $\tilde{\boldsymbol{I}}_+, \tilde{\boldsymbol{I}}_- \in \mathcal{I}$, which satisfy $\mathcal{L}(\tilde{\boldsymbol{I}}_+,\lambda^\star) = \mathcal{L}(\tilde{\boldsymbol{I}}_-,\lambda^\star) = g(\lambda^\star)$, and $f_P(\tilde{\boldsymbol{I}}_+) \geq 0$, $f_P(\tilde{\boldsymbol{I}}_-) \leq 0$ [18], [19]. Note that $\lambda^\star$ can be expressed as $\lambda^\star = \frac{f_D(\tilde{\boldsymbol{I}}_+)-f_D(\tilde{\boldsymbol{I}}_-)}{f_P(\tilde{\boldsymbol{I}}_-)-f_P(\tilde{\boldsymbol{I}}_+)}$; moreover, the corresponding $\tilde{\boldsymbol{I}}_-$ is a feasible solution to (P4). Motivated by this, the algorithm works by iteratively checking a series of potential $\boldsymbol{I}_+$'s and $\boldsymbol{I}_-$'s as well as $\lambda = \frac{f_D(\boldsymbol{I}_+)-f_D(\boldsymbol{I}_-)}{f_P(\boldsymbol{I}_-)-f_P(\boldsymbol{I}_+)}$ by leveraging the supergradient of $g(\lambda)$. Specifically, define $\boldsymbol{I}^\star(\lambda) \triangleq \arg\min_{\boldsymbol{I}\in\mathcal{I}} \mathcal{L}(\boldsymbol{I},\lambda)$, which can be efficiently obtained by finding the *shortest path* from U_0 to U_F in G with respect to the weights $W_D + \lambda W_P$ via e.g., the Dijkstra algorithm [14]. It can be shown that $f_P(\boldsymbol{I}^\star(\lambda))$ is a supergradient of $g(\lambda)$ at λ, since $g(\lambda') = f_D(\boldsymbol{I}^\star(\lambda'))+\lambda' f_P(\boldsymbol{I}^\star(\lambda')) \leq f_D(\boldsymbol{I}^\star(\lambda))+\lambda' f_P(\boldsymbol{I}^\star(\lambda)) = g(\lambda)+(\lambda'-\lambda) f_P(\boldsymbol{I}^\star(\lambda))$ holds for all λ'. Therefore, if $f_P(\boldsymbol{I}^\star(\lambda)) < 0$, we have $0 \leq \lambda^\star < \lambda$, and otherwise $\lambda^\star \geq \lambda$.

Based on the above, we first obtain $\boldsymbol{I}^\star(0) = \arg\min_{\boldsymbol{I}\in\mathcal{I}} f_D(\boldsymbol{I})$ and $\boldsymbol{I}^\star(\infty) = \arg\min_{\boldsymbol{I}\in\mathcal{I}} f_P(\boldsymbol{I})$ via shortest path algorithms, which correspond to the "best" paths with respect to the objective function and constraint function of (P4), respectively. Note that if $f_P(\boldsymbol{I}^\star(0)) \leq 0$, the optimal solution to (P4) is readily obtained as $\boldsymbol{I}^\star(0)$. Then, by setting $\boldsymbol{I}_+ = \boldsymbol{I}^\star(0)$, $\boldsymbol{I}_- = \boldsymbol{I}^\star(\infty)$, we consider $\lambda = \frac{f_D(\boldsymbol{I}_+)-f_D(\boldsymbol{I}_-)}{f_P(\boldsymbol{I}_-)-f_P(\boldsymbol{I}_+)}$ and obtain $\boldsymbol{I}^\star(\lambda)$ via shortest path algorithms. If $\mathcal{L}(\boldsymbol{I}^\star(\lambda),\lambda) = \mathcal{L}(\boldsymbol{I}_+,\lambda) = \mathcal{L}(\boldsymbol{I}_-,\lambda)$, then λ is the optimal solution to (P4-Dual), and $\boldsymbol{I}_-$ is the obtained

Algorithm 1: Proposed Algorithm for Problem (P4)

Input: $\bar{d}$, $\boldsymbol{u}_0$, $\boldsymbol{u}_F$, $\{\boldsymbol{g}_m\}_{m=1}^M$, K
Output: $\tilde{\boldsymbol{I}}$

Construct a graph $G = (V, E)$ based on (47), (48), (49) and (51).
Obtain $\boldsymbol{I}^\star(0) = \arg\min_{\boldsymbol{I}\in\mathcal{I}} f_D(\boldsymbol{I})$ and $\boldsymbol{I}^\star(\infty) = \arg\min_{\boldsymbol{I}\in\mathcal{I}} f_P(\boldsymbol{I})$ via Dijkstra algorithm.
if $f_P(\boldsymbol{I}^\star(0)) \leq 0$ **then**
    Obtain $\tilde{\boldsymbol{I}} = \boldsymbol{I}^\star(0)$, which is the optimal solution to (P4).
else
    Set $\boldsymbol{I}^+ = \boldsymbol{I}^\star(0)$, $\boldsymbol{I}^- = \boldsymbol{I}^\star(\infty)$, and $\lambda = \frac{f_D(\boldsymbol{I}_+) - f_D(\boldsymbol{I}_-)}{f_P(\boldsymbol{I}_-) - f_P(\boldsymbol{I}_+)}$.
    while $\mathcal{L}(\boldsymbol{I}^\star(\lambda), \lambda) \neq \mathcal{L}(\boldsymbol{I}_+, \lambda)$ **do**
        If $f_P(\boldsymbol{I}^\star(\lambda)) < 0$, set $\boldsymbol{I}_- = \boldsymbol{I}^\star(\lambda)$; otherwise, set $\boldsymbol{I}_+ = \boldsymbol{I}^\star(\lambda)$.
        Set $\lambda = \frac{f_D(\boldsymbol{I}_+) - f_D(\boldsymbol{I}_-)}{f_P(\boldsymbol{I}_-) - f_P(\boldsymbol{I}_+)}$.
    end
    Set $\lambda^\star = \lambda$. Obtain $\tilde{\boldsymbol{I}}_1, ..., \tilde{\boldsymbol{I}}_K$ as the K-shortest paths in graph G from U_0 to U_F with respect to weights $W_D + \lambda^\star W_P$'s via Yen's algorithm.
    Obtain $\tilde{\boldsymbol{I}} = \arg \min_{\boldsymbol{I}\in\{\boldsymbol{I}_-, \tilde{\boldsymbol{I}}_1, ..., \tilde{\boldsymbol{I}}_K\}, f_P(\boldsymbol{I})\leq 0} f_D(\boldsymbol{I})$.
end

feasible solution for (P4). Otherwise, we set $\boldsymbol{I}_- = \boldsymbol{I}^\star(\lambda)$ if $f_P(\boldsymbol{I}^\star(\lambda)) < 0$, or $\boldsymbol{I}_+ = \boldsymbol{I}^\star(\lambda)$ if $f_P(\boldsymbol{I}^\star(\lambda)) \geq 0$, and query another λ based on the aforementioned procedure, until the optimal λ is found. Note that as the algorithm iterates, it can be shown that the dual objective value $g(\lambda)$ is non-decreasing due to the supergradient-based iteration policy; moreover, the objective value of the primal problem with the solution $\boldsymbol{I}_-$, $f_D(\boldsymbol{I}_-)$, is non-increasing, since λ generally decreases with the updates of $\boldsymbol{I}_-$, and it holds that $f_D(\boldsymbol{I}^\star(\lambda)) \leq f_D(\boldsymbol{I}^\star(\lambda'))$ if $\lambda \leq \lambda'$ [18], [19], [22]. Therefore, the algorithm is guaranteed to converge, for which the worst-case complexity is given by $\mathcal{O}(M^4 \log^2 M)$ [18], [19], [22].

Last, notice that the obtained $\boldsymbol{I}_-$ is not necessarily the optimal solution to (P4) due to the non-zero duality gap, and several heuristic methods have been proposed in [18], [19] to refine the solution, among which we adopt the K-shortest paths based method proposed in [18] in this paper. Specifically, with the optimal $\lambda^\star$, K paths from U_0 to U_F in graph G that yields the first K smallest values of $W_D + \lambda^\star W_P$ are obtained via the Yen's algorithm [20], which are denoted by $\tilde{\boldsymbol{I}}_1, ..., \tilde{\boldsymbol{I}}_K$. The final solution is then selected from $\{\boldsymbol{I}_-, \tilde{\boldsymbol{I}}_1, ..., \tilde{\boldsymbol{I}}_K\}$ as the one feasible for (P4) and yielding the minimum objective value. The overall algorithm is summarized in Algorithm 1. Note that the obtained solution in Algorithm 1 is always feasible for (P4), whose performance

generally improves as the value of K increases. Moreover, since finding the K-shortest paths requires complexity of $\mathcal{O}(M^3K)$ [20], the overall worst-case complexity for Algorithm 1 is $\mathcal{O}(M^4\log^2 M + M^3K)$. For more detailed explanations and rigorous convergence analysis of this algorithm, please refer to [18], [19], [22].

Finally, recall from Section VI-A that the worst-case complexity for obtaining the optimal $\{\boldsymbol{u}_i^{\mathrm{I}}, \boldsymbol{u}_i^{\mathrm{O}}\}_{i=1}^N$ with given $\boldsymbol{I}$ is $\mathcal{O}(M^{3.5})$, thus the overall worst-case complexity of the proposed approach for finding a suboptimal solution to (P3) is $\mathcal{O}(M^4\log^2 M + M^3K)$, which is significantly reduced as compared to $\mathcal{O}(M^{3.5}M!)$ for finding the optimal solution when M is large.

VII. Special Case with $\alpha \to \infty$

Note that the proposed methods for checking the feasibility as well as finding optimal and suboptimal solutions of (P3) in the preceding sections are applicable to the general case with any given $\alpha \geq 0$, thus can also be applied to the special case with $\alpha \to \infty$ by approximating α with a sufficiently large number. However, this may require additional down-scaling of the edge weights in the graph G to avoid arithmetic overflow due to the large α. Motivated by this issue as well as the unique structures of (P3) with $\alpha \to \infty$, we devise alternative algorithms with lower complexity for this special case in this section. Specifically, note that with $\alpha \to \infty$, the constraint in (38) can be rewritten as

$$\max_{i=1,\ldots,N+1} \|\boldsymbol{u}_i^{\mathrm{I}} - \boldsymbol{u}_{i-1}^{\mathrm{O}}\| \leq V_{\max}\bar{f}_{\mathrm{O},\infty}, \tag{57}$$

by leveraging the properties of the generalized mean and noting that $\lim\limits_{\alpha\to\infty} \frac{1}{(\alpha+1)^{\frac{1}{\alpha+1}}} = 1$ holds. It is worth noting that compared to (38) for the general case where all $\boldsymbol{u}_i^{\mathrm{I}}$'s and $\boldsymbol{u}_i^{\mathrm{O}}$'s are coupled, (57) for the special case of $\alpha \to \infty$ is in a simpler form, which is equivalent to $N+1$ independent constraints on each $\|\boldsymbol{u}_i^{\mathrm{I}} - \boldsymbol{u}_{i-1}^{\mathrm{O}}\|$. With this simplified constraint, (P3) can be more efficiently solved, as shown next.

A. Feasibility Check with $\alpha \to \infty$

In this subsection, we check the feasibility of (P3) by solving (P3-F) with $\alpha \to \infty$. In this case, the minimum outage cost with given $\boldsymbol{I}$ shown in (42) can be rewritten as

$$f_{\mathrm{O},\infty}^{\star}(\boldsymbol{I}) = \lim_{\alpha\to\infty} f_{\mathrm{O},\alpha}^{\star}(\boldsymbol{I}) = \frac{1}{V_{\max}} \max\left\{\|\boldsymbol{u}_0 - \boldsymbol{g}_{I_1}\| - \bar{d}, \|\boldsymbol{u}_F - \boldsymbol{g}_{I_N}\| - \bar{d}, \max_{i\in\{2,\ldots,N\}} \|\boldsymbol{g}_{I_i} - \boldsymbol{g}_{I_{i-1}}\| - 2\bar{d}, 0\right\}. \tag{58}$$

Consequently, for the case of $\alpha \to \infty$, (P3) is feasible if and only if there exists an $\boldsymbol{I}$ which satisfies (37), (39), as well as $\|\boldsymbol{u}_0 - \boldsymbol{g}_{I_1}\| - \bar{d} \leq V_{\max}\bar{f}_{\mathrm{O},\infty}$, $\|\boldsymbol{g}_{I_i} - \boldsymbol{g}_{I_{i-1}}\| - 2\bar{d} \leq V_{\max}\bar{f}_{\mathrm{O},\infty}, \forall i \in \{2, ..., N\}$, and $\|\boldsymbol{u}_F - \boldsymbol{g}_{I_N}\| - \bar{d} \leq V_{\max}\bar{f}_{\mathrm{O},\infty}$. Based on this, we provide a new graph based solution of (P3-F). Specifically, we construct a new undirected graph denoted by $G_\infty = (V_\infty, E_\infty)$. The vertex set of G_∞ is given by

$$V_\infty = \{U_0, G_1, G_2, ..., G_M, U_F\}. \tag{59}$$

The edge set of G_∞ is given by

$$\begin{aligned} E_\infty =& \{(U_0, G_m) : \|\boldsymbol{u}_0 - \boldsymbol{g}_m\| - \bar{d} \leq V_{\max}\bar{f}_{\mathrm{O},\infty}, m \in \mathcal{M}\} \\ & \cup \{(G_m, G_n) : \|\boldsymbol{g}_m - \boldsymbol{g}_n\| - 2\bar{d} \leq V_{\max}\bar{f}_{\mathrm{O},\infty}, m, n \in \mathcal{M}, m \neq n\} \\ & \cup \{(U_F, G_m) : \|\boldsymbol{u}_F - \boldsymbol{g}_m\| - \bar{d} \leq V_{\max}\bar{f}_{\mathrm{O},\infty}, m \in \mathcal{M}\}. \end{aligned} \tag{60}$$

With the constructed graph G_∞, (P3) is feasible if and only U_0 and U_F in G_∞ are *connected* [14], and $\boldsymbol{I}$ is a feasible solution to (P3) if and only if it corresponds to a path in G_∞ from U_0 to U_F. Hence, the feasibility of (P3) can be checked by constructing G_∞ with complexity of $\mathcal{O}(M^2)$, and checking the connectivity between U_0 and U_F in G_∞ via e.g., breadth-first search with worst-case complexity of $\mathcal{O}(|V_\infty| + |E_\infty|) = \mathcal{O}(M^2)$ [14], thus requiring an overall complexity of $\mathcal{O}(M^2)$. Note that although in the same order $\mathcal{O}(M^2)$, the complexity for checking the feasibility of (P3) for the special case of $\alpha \to \infty$ is in general smaller than that for the general case with finite $\alpha \geq 0$, since $|V_\infty| + |E_\infty| \leq |E| + |V| \log |V|$ holds for the constructed G and G_∞.

B. Proposed Solution to (P3) with $\alpha \to \infty$

1) Optimal Solution: Note that with the constraint in (38) replaced by that in (57) for the case of $\alpha \to \infty$, (P3) is still a convex problem with given $\boldsymbol{I}$, which can be solved via CVX with worst-case complexity of $\mathcal{O}(M^{3.5})$. Therefore, similar to the general case of $\alpha \geq 0$, the optimal solution to (P3) can be found by finding all paths in G_∞ from U_0 to U_F as well as the corresponding optimal $\{\boldsymbol{u}_i^{\mathrm{I}}, \boldsymbol{u}_i^{\mathrm{O}}\}_{i=1}^N$'s and selecting the one with the minimum objective value, for which the worst-case complexity is $\mathcal{O}(M^{3.5}M!)$.

2) Suboptimal Solution: Similar to the general case of $\alpha \geq 0$ discussed in Section VI-B, an approximate solution of $\boldsymbol{I}$ to (P3) with $\alpha \to \infty$ can be obtained by substituting (43)–(46) into (P3) and solving (P3) with the objective value replaced by its upper bound shown in (50), for

which we propose a new graph based solution in this special case. Consider the same graph $G_\infty = (V_\infty, E_\infty)$ as constructed in Section VII-A. We further consider a set of weights for G_∞:

$$W_\infty(U_0, G_m) = \|\boldsymbol{u}_0 - \boldsymbol{g}_m\|,\ W_\infty(U_F, G_m) = \|\boldsymbol{u}_F - \boldsymbol{g}_m\|,$$
$$W_\infty(G_m, G_n) = \|\boldsymbol{g}_m - \boldsymbol{g}_n\|, \quad m, n \in \mathcal{M}, m \neq n. \tag{61}$$

With the constructed G_∞, the aforementioned problem is equivalent to finding the *shortest path* from U_0 to U_F in G_∞ with respect to the weights W_∞'s, which can be efficiently solved via e.g., the Dijkstra algorithm with worst-case complexity of $\mathcal{O}(|E_\infty| + |V_\infty| \log |V_\infty|) = \mathcal{O}(M^2)$ [14]. By further noting that constructing the graph G_∞ also requires complexity of $\mathcal{O}(M^2)$, the overall complexity for finding a suboptimal solution of $\boldsymbol{I}$ is thus $\mathcal{O}(M^2)$. By noting that the worst-case complexity for obtaining the optimal waypoint locations with the given $\boldsymbol{I}$ is $\mathcal{O}(M^{3.5})$, the overall worst-case complexity for finding a suboptimal solution to (P3) with $\alpha \to \infty$ is $\mathcal{O}(M^{3.5})$, which is smaller compared to that for the general case with finite $\alpha \geq 0$ given by $\mathcal{O}(M^4 \log^2 M + M^3 K)$.

VIII. Numerical Examples

In this section, we provide numerical examples to evaluate our proposed trajectory designs under outage duration constraints. We consider M GBSs that are randomly distributed in a D km $\times$ D km region, with $D = 10$. The altitude of the UAV and each GBS are set as $H = 90$ m and $H_{\rm G} = 12.5$ m, respectively. The maximum UAV speed is set as $V_{\max} = 50$ m/s. The reference SNR at distance $d_0 = 1$ m is set as $\gamma_0 = \frac{P\beta_0}{\sigma^2} = 80$ dB. For Algorithm 1 in our proposed suboptimal design, we set $K = 6$ in the K-shortest paths procedure.

A. Performance and Complexity of Proposed Trajectory Designs

In this subsection, we evaluate the performance and complexity of the proposed trajectory designs with given α. For comparison, we consider a *DP-based* trajectory design according to the *myopic policy* [23] as a benchmark scheme.[4] In the DP-based design, the D km$\times D$ km area is quantized to a grid with granularity Δ m, which specifies the set of $(Q+1)\times(Q+1)$ possible UAV locations during its flight, with $Q = \frac{1000D}{\Delta}$.[5] The trajectory is then found in a recursive manner by iteratively updating the "best" last grid point (from a set of neighboring points within distance n_r

[4]To the best of the authors' knowledge, there has been no prior work on solving the considered problem via other more sophisticated DP-based methods (e.g., policy/value function approximations [23]), which are not considered in this paper due to high complexity, thus will be left as future work directions.

[5]We assume that $Q = \frac{1000D}{\Delta}$ is an integer without loss of generality.

m) before the UAV arrives at each grid point. Specifically, in each iteration, a neighboring point (p_n, q_n) is stored for each point (p, q) that denotes the "best" last grid point for the UAV to travel from U_0 to the location with grid coordinate (p, q), where $p, q, p_n, q_n \in \{0, ..., Q\}$. Moreover, we construct two matrices $\boldsymbol{T}$ and $\boldsymbol{F}$ both of size $(Q+1) \times (Q+1)$, in which each (p, q)th entry $T_{p,q}$ and $F_{p,q}$ represent the time needed to travel from U_0 to (p, q) and the incurred outage cost so far, i.e., $\left(\int_0^{T_{p,q}} (t - t_{\mathrm{N}}(t))^{\alpha} dt\right)^{\frac{1}{\alpha+1}}$, respectively, following the current "best" trajectory specified by (p_n, q_n)'s. In each iteration, the "best" neighboring point (p_n, q_n) for each (p, q) is updated such that $T_{p,q}$ is minimized, yet the outage cost constraint in (15) is not violated, namely,

$$(p_n, q_n) = \arg \min_{\substack{\left\{(p_n,q_n): \|[p_n,q_n]-[p,q]\|\Delta \le n_r, \\ \left(F_{p_n,q_n}^{\alpha+1} + \int_{T_{p_n,q_n}}^{T_{p,q}} (t - t_{\mathrm{N}}(t))^{\alpha} dt\right)^{\frac{1}{\alpha+1}} \le \bar{f}_{\mathrm{O},\alpha}\right\}}} T_{p_n,q_n} + \frac{\|[p_n, q_n] - [p, q]\|\Delta}{V_{\max}}. \tag{62}$$

The matrices $\boldsymbol{T}$ and $\boldsymbol{F}$ are then updated accordingly after each iteration, and the algorithm terminates if no change is made to $\boldsymbol{T}$ and $\boldsymbol{F}$. Note that a similar method has been adopted in [11] for the special case of $\alpha \to \infty$, thus more details are omitted in this paper for brevity.

For illustration, we take the example of $M = 7$ and a random realization of GBSs' locations shown in Fig. 6. The UAV's initial and final locations projected on the horizontal plane are set as $\boldsymbol{u}_0 = [1 \text{ km}, 1 \text{ km}]^T$ and $\boldsymbol{u}_F = [9 \text{ km}, 9 \text{ km}]^T$, respectively. We consider two values of α, namely, $\alpha = 0$ and $\alpha \to \infty$. The minimum receive SNR target is set as $\bar{\rho} = 19$ dB. Under the above setup, we first minimize the outage cost $f_{\mathrm{O},\alpha}$ based on the results in Section V and Section VII-A, which are obtained as $\bar{f}_{\mathrm{O},0,\min} = 75.4304$ and $\bar{f}_{\mathrm{O},\infty,\min} = 42.6041$, respectively. Then, we obtain an upper bound on the outage cost $f_{\mathrm{O},\alpha}$ with the straight-flight (SF) trajectory from U_0 to U_F, which are $\bar{f}_{\mathrm{O},0,\mathrm{SF}} = 135.0269$ and $\bar{f}_{\mathrm{O},\infty,\mathrm{SF}} = 135.0269$. Note that the SF trajectory achieves the minimum mission completion time T, thus the optimal solution to (P1) with any $\bar{f}_{\mathrm{O},\alpha} > \bar{f}_{\mathrm{O},\alpha,\mathrm{SF}}$ can be easily shown to be the SF trajectory. Hence, we evaluate our proposed trajectory designs for $\bar{f}_{\mathrm{O},\alpha} \in [\bar{f}_{\mathrm{O},\alpha,\min}, \bar{f}_{\mathrm{O},\alpha,\mathrm{SF}}]$ in the following.

Then, we compare the performance and complexity of our proposed trajectory designs in Section VI and Section VII versus the DP-based trajectory. For the DP-based design, we set $\Delta = 200$ or 500 m, and $n_r = 1000$ m. In Fig. 4, we show the mission completion time T versus the outage cost constraint $\bar{f}_{\mathrm{O},\alpha}$ for the proposed optimal and suboptimal solutions as compared to the DP-based solution with $\Delta = 200$ or 500. It is observed that for both settings of α, our proposed suboptimal solution achieves close or even the same performance as the optimal solution, thus validating the efficacy of the bounding and approximation techniques applied for

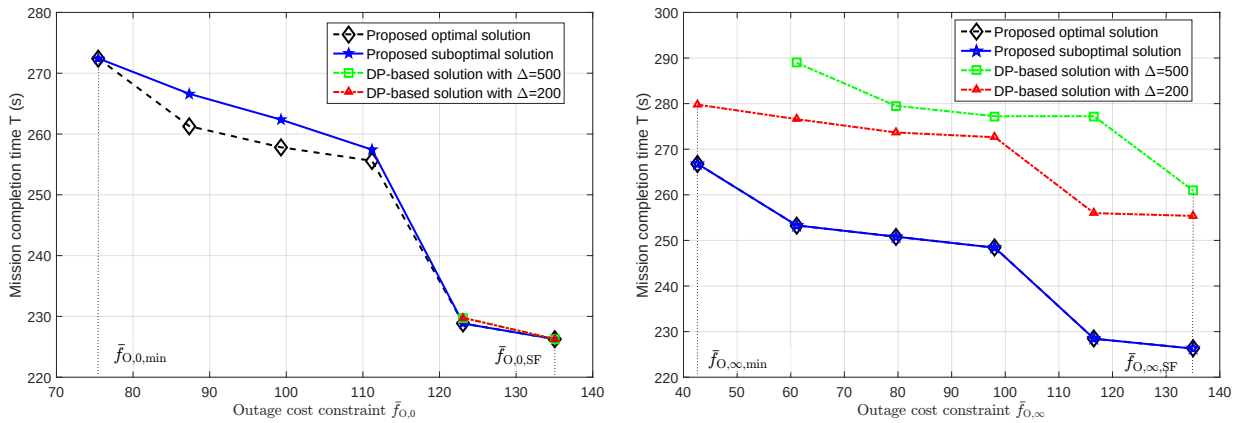

(a) $\alpha = 0$ (b) $\alpha \to \infty$

Fig. 4. Mission completion time T versus $\bar{f}_{\mathrm{O},\alpha}$ for different trajectory designs.

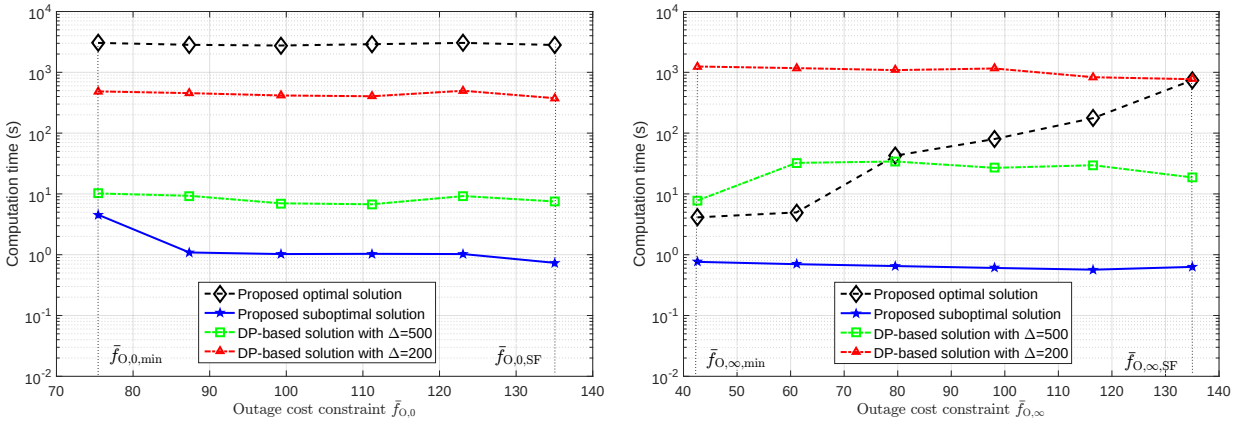

(a) $\alpha = 0$ (b) $\alpha \to \infty$

Fig. 5. Computation time versus $\bar{f}_{\mathrm{O},\alpha}$ for different trajectory designs.

solving (P3) shown in Section VI-B and VII-B2. Moreover, note that the DP-based solutions with both $\Delta = 500$ and $\Delta = 200$ are infeasible for the first four sample points of $\bar{f}_{\mathrm{O},\alpha}$ for the case of $\alpha = 0$; while for the case of $\alpha \to \infty$, the DP-based solution with $\Delta = 500$ is infeasible for the first sample point. This is because with the myopic policy, the DP-based design cannot take into account the future outage events in the UAV trajectory, thus is not guaranteed to find a feasible solution that satisfies the *overall* outage cost constraint. In addition, it is observed that for both $\alpha = 0$ and $\alpha \to \infty$, the DP-based solution with $\Delta = 200$ outperforms that with $\Delta = 500$, since smaller granularity results in finer-grained UAV locations and thus better performance. Furthermore, both DP-based solutions are outperformed by our proposed solutions. This is because our proposed solutions jointly optimize all UAV locations along its flight, thus being more effective than the myopic based DP; moreover, with the optimal trajectory structure given in Proposition 2, our proposed solutions only need to find critical parameters such as the

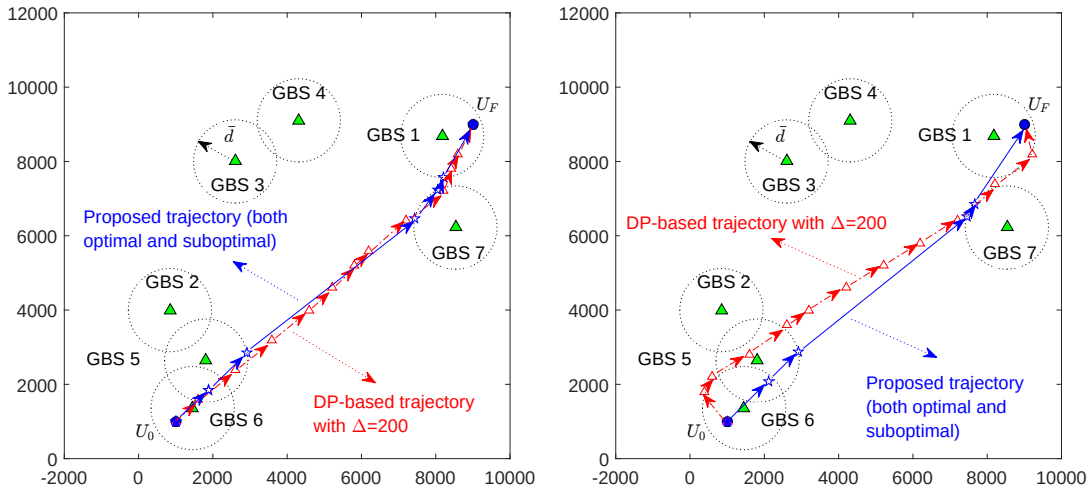

(a) $\alpha = 0$ (b) $\alpha \to \infty$

Fig. 6. Comparison of different trajectory designs with $\bar{f}_{\mathrm{O},\alpha} = \bar{f}_{\mathrm{O},\alpha,\min} + \frac{4}{5}(\bar{f}_{\mathrm{O},\alpha,\mathrm{SF}} - \bar{f}_{\mathrm{O},\alpha,\min})$.

GBS-UAV association sequence and the waypoint locations, thus being more efficient than the DP-based solutions which require quantization of the entire area of interest to check all possible UAV locations.

Next, we show in Fig. 5 the required computation time for the different trajectory design solutions.[6] It is observed that the computation time for DP-based solutions increases as Δ decreases, due to the rapidly enlarged state-space set. In contrast, our proposed suboptimal solution requires much less computation time than the DP-based solutions as well as the proposed optimal solution; thus it is a practically appealing solution from both performance and complexity considerations. Last, we consider $\bar{f}_{\mathrm{O},\alpha} = \bar{f}_{\mathrm{O},\alpha,\min} + \frac{4}{5}(\bar{f}_{\mathrm{O},\alpha,\mathrm{SF}} - \bar{f}_{\mathrm{O},\alpha,\min})$ (the fifth sample point of $\bar{f}_{\mathrm{O},\alpha}$ in Fig. 4) and illustrate in Fig. 6 the proposed and DP-based (with $\Delta = 200$) trajectories. It can be observed that our proposed trajectory is generally different from the DP-based trajectory.

B. Proposed Trajectory Designs with Different α and SNR Target $\bar{\rho}$

In this subsection, we compare the performance of our proposed suboptimal trajectory designs with different values of α and the SNR target $\bar{\rho}$, under the minimum achievable outage cost constraint. We take the example of $M = 15$ and a random realization of GBSs' locations shown in Fig. 8. The UAV's initial and final locations projected on the horizontal plane are set as $\boldsymbol{u}_0 = [2\ \mathrm{km}, 2\ \mathrm{km}]^T$ and $\boldsymbol{u}_F = [8\ \mathrm{km}, 8\ \mathrm{km}]^T$, respectively. We consider three values of α: $\alpha = 0$, $\alpha = 1$, and $\alpha \to \infty$. To begin with, we show in Fig. 7 the minimum achievable

[6]All the computations are executed by MATLAB on a computer with an Intel Core i5 3.40-GHz CPU and 8 GB of memory.

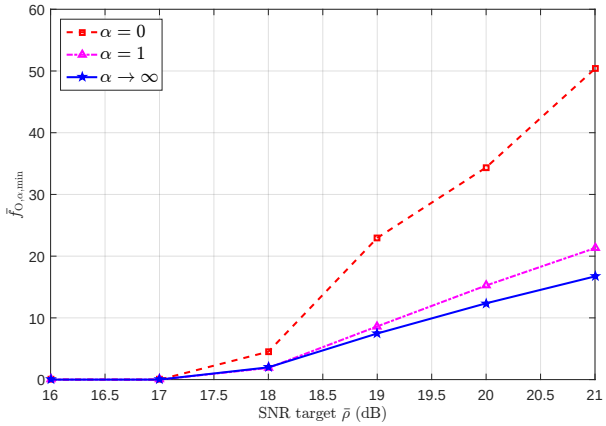

Fig. 7. Minimum outage cost $\bar{f}_{\mathrm{O},\alpha,\min}$ versus SNR target $\bar{\rho}$.

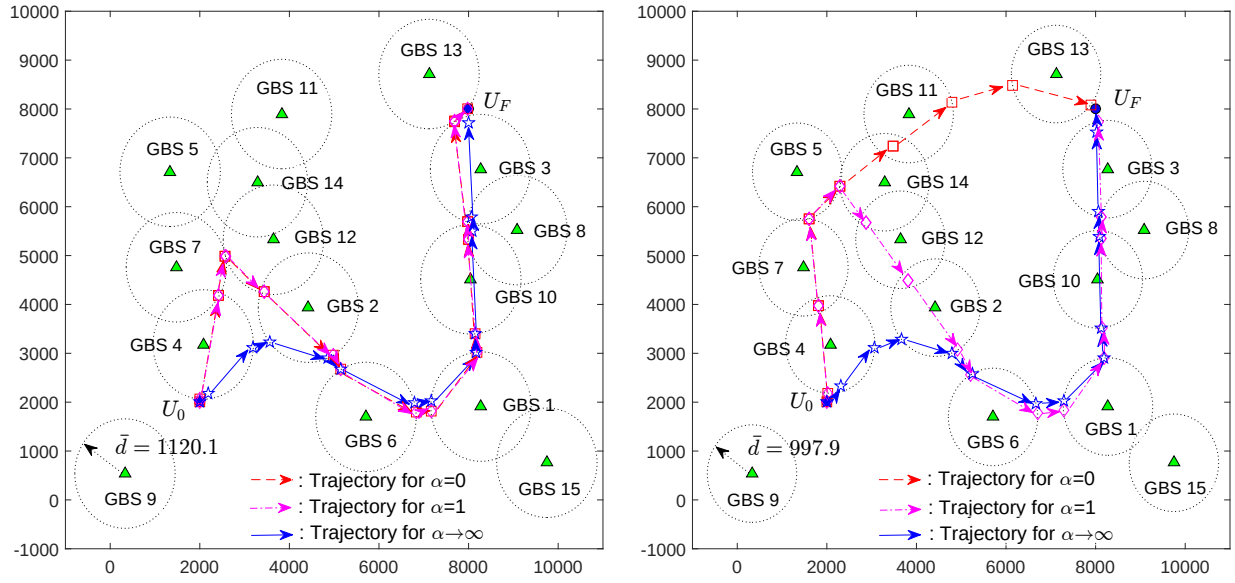

(a) $\bar{\rho} = 19$ dB (b) $\bar{\rho} = 20$ dB

Fig. 8. Comparison of proposed trajectory designs with different α under minimum outage cost $\bar{f}_{\mathrm{O},\alpha} = \bar{f}_{\mathrm{O},\alpha,\min}$.

outage cost $\bar{f}_{\mathrm{O},\alpha,\min}$ for different values of α versus the SNR target $\bar{\rho}$. It is observed that for all α, $\bar{f}_{\mathrm{O},\alpha,\min}$ increases as $\bar{\rho}$ increases, since a larger $\bar{\rho}$ corresponds to a smaller communication range $\bar{d}$, and consequently a more stringent constraint in (6) for non-outage communication. Moreover, the increase in $\bar{f}_{\mathrm{O},\alpha,\min}$ with $\bar{\rho}$ is more pronounced as α decreases. This is because as α decreases, outage durations tend to be more equally important in the outage cost function $f_{\mathrm{O},\alpha}$, thus resulting in a more significant increase in $\bar{f}_{\mathrm{O},\alpha,\min}$.

Next, we fix two SNR targets as $\bar{\rho} = 19$ dB and $\bar{\rho} = 20$ dB, and show their corresponding trajectory designs with different α under the minimum outage cost constraint specified by $f_{\mathrm{O},\alpha} \leq \bar{f}_{\mathrm{O},\alpha,\min}$ in Fig. 8(a) and Fig. 8(b), respectively. It is observed that for each $\bar{\rho}$, the corresponding trajectories to different α are quite different, due to the distinct structures of the outage cost

function $f_{\mathrm{O},\alpha}$. For instance, under the setup of $\bar{\rho} = 20$ dB, the trajectory for $\alpha = 0$ consists of a handover from GBS 11 to GBS 13, which results in a large outage duration; while that for $\alpha \to \infty$ consists of more handovers that incur outage, but each of them has a much smaller duration. Moreover, it is interesting to notice that the trajectory for $\alpha = 1$ strikes a balance between the two other cases. In addition, it is observed that the trajectories for $\alpha = 0$ and $\alpha = 1$ under the two SNR targets are also substantially different, due to the different communication range $\bar{d}$ (i.e., $\bar{d} = 1120.1$ for $\bar{\rho} = 19$ dB and $\bar{d} = 997.9$ for $\bar{\rho} = 20$ dB). Therefore, the trajectory design is critically dependent on the practical choice of α and the required SNR target $\bar{\rho}$.

IX. Conclusions

This paper studies the trajectory design for cellular-connected UAV under delay-limited communications, where a minimum receive SNR target is considered for non-outage UAV communications. We propose a general outage cost function to characterize the effect of outage durations in the UAV's flight to the communication performance in different applications. We formulate the UAV trajectory optimization problem to minimize the UAV's mission completion time from an initial location to a final location, subject to a constraint on the maximum tolerable outage cost in the flight. By exploiting the optimal structure of the trajectory solution, we apply graph theory and convex optimization techniques to devise efficient algorithms to check the problem feasibility and find both optimal and low-complexity suboptimal solutions. Numerical examples validate the efficacy of our proposed designs and show its performance and complexity advantages against DP-based method.

Appendix

A. Proof of Proposition 1

First, for any feasible solution $(\tilde{T}, \{\tilde{\boldsymbol{u}}(t), 0 \le t \le \tilde{T}\})$ to (P1), we can always construct a GBS-UAV association sequence $\tilde{\boldsymbol{I}} = [\tilde{I}_1, ..., \tilde{I}_{\tilde{N}}]^{\tilde{N}}$ and a set of critical time instants $\{\tilde{t}_i^{\mathrm{I}}, \tilde{t}_i^{\mathrm{O}}\}_{i=1}^{\tilde{N}}$ based on their definitions presented in Section IV, which satisfy the constraints in (22)–(26). Moreover, it follows from (18) and (19) that $\left(\sum_{i=1}^{\tilde{N}+1} \frac{(\tilde{t}_i^{\mathrm{I}} - \tilde{t}_{i-1}^{\mathrm{O}})^{\alpha+1}}{\alpha+1}\right)^{\frac{1}{\alpha+1}} = \left(\int_0^{\tilde{T}} (t - \tilde{t}_{\mathrm{N}}(t))^{\alpha} dt\right)^{\frac{1}{\alpha+1}} \le \bar{f}_{\mathrm{O},\alpha}$ holds, with $\tilde{t}_{\mathrm{N}}(t)$ given in (6) by substituting $\tilde{T}$ and $\{\tilde{\boldsymbol{u}}(t), 0 \le t \le \tilde{T}\}$, thus $(\tilde{\boldsymbol{I}}, \{\tilde{t}_i^{\mathrm{I}}, \tilde{t}_i^{\mathrm{O}}\}_{i=1}^{\tilde{N}}, \tilde{T}, \{\tilde{\boldsymbol{u}}(t), 0 \le t \le \tilde{T}\})$ is a feasible solution to (P2) with the same objective value as (P1) given the solution $(\tilde{T}, \{\tilde{\boldsymbol{u}}(t), 0 \le t \le \tilde{T}\})$. Hence, the optimal value of (P2) is no larger than that of (P1). On the other hand, for any feasible solution $(\tilde{\boldsymbol{I}}, \{\tilde{t}_i^{\mathrm{I}}, \tilde{t}_i^{\mathrm{O}}\}_{i=1}^{\tilde{N}}, \tilde{T}, \{\tilde{\boldsymbol{u}}(t), 0 \le t \le \tilde{T}\})$ to (P2), it can be

shown from (6) and (22) that $\left(\int_0^{\tilde{T}}(t-\tilde{t}_{\rm N}(t))^{\alpha}dt\right)^{\frac{1}{\alpha+1}} \leq \left(\sum_{i=1}^{\tilde{N}+1}\frac{(\tilde{t}_i^{\rm I}-\tilde{t}_{i-1}^{\rm O})^{\alpha+1}}{\alpha+1}\right)^{\frac{1}{\alpha+1}} \leq \bar{f}_{{\rm O},\alpha}$ holds, thus $(\tilde{T},\{\tilde{\boldsymbol{u}}(t),0\leq t\leq\tilde{T}\})$ is a feasible solution to (P1) and achieves the same objective value as (P2) with the solution $(\tilde{\boldsymbol{I}},\{\tilde{t}_i^{\rm I},\tilde{t}_i^{\rm O}\}_{i=1}^{\tilde{N}},\tilde{T},\{\tilde{\boldsymbol{u}}(t),0\leq t\leq\tilde{T}\})$. Hence, the optimal value of (P1) is no larger than that of (P2). Therefore, (P1) and (P2) have the same optimal value, which completes the proof of Proposition 1.

B. Proof of Proposition 2

We prove Proposition 2 by showing that for any feasible solution to (P2) that does not satisfy the conditions in (28)–(31), denoted as $(\tilde{\boldsymbol{I}},\{\tilde{t}_i^{\rm I},\tilde{t}_i^{\rm O}\}_{i=1}^{\tilde{N}},\tilde{T},\{\tilde{\boldsymbol{u}}(t),0\leq t\leq\tilde{T}\})$, we can always find an alternative feasible solution to (P2) denoted as $(\tilde{\boldsymbol{I}},\{t_i^{\rm I},t_i^{\rm O}\}_{i=1}^{\tilde{N}},T,\{\boldsymbol{u}(t),0\leq t\leq T\})$ that satisfies the conditions in (28)–(31) and achieves a smaller objective value of (P2) compared to the solution $(\tilde{\boldsymbol{I}},\{\tilde{t}_i^{\rm I},\tilde{t}_i^{\rm O}\}_{i=1}^{\tilde{N}},\tilde{T},\{\tilde{\boldsymbol{u}}(t),0\leq t\leq\tilde{T}\})$. Specifically, we first construct the same set of waypoint locations in $\boldsymbol{u}(t)$ as those in $\tilde{\boldsymbol{u}}(t)$, i.e., $\boldsymbol{u}_i^{\rm I}=\tilde{\boldsymbol{u}}(\tilde{t}_i^{\rm I}),\boldsymbol{u}_i^{\rm O}=\tilde{\boldsymbol{u}}(\tilde{t}_i^{\rm O}),i=1,...,\tilde{N}$. Then, we construct $\{t_i^{\rm I},t_i^{\rm O}\}_{i=1}^{\tilde{N}}$, T and $\{\boldsymbol{u}(t),0\leq t\leq T\}$ according to (28)–(31) based on the constructed $\{\boldsymbol{u}_i^{\rm I},\boldsymbol{u}_i^{\rm O}\}_{i=1}^{\tilde{N}}$. Note that since $(\tilde{\boldsymbol{I}},\{\tilde{t}_i^{\rm I},\tilde{t}_i^{\rm O}\}_{i=1}^{\tilde{N}},\tilde{T},\{\tilde{\boldsymbol{u}}(t),0\leq t\leq\tilde{T}\})$ satisfies the constraints in (22), it follows that $\boldsymbol{u}_i^{\rm I}\in\mathcal{C}_{I_i}$ and $\boldsymbol{u}_i^{\rm O}\in\mathcal{C}_{I_i}$ hold for all $i\in\{1,...,N\}$. Therefore, the constraints in (22) are also satisfied with the solution $(\tilde{\boldsymbol{I}},\{t_i^{\rm I},t_i^{\rm O}\}_{i=1}^{\tilde{N}},T,\{\boldsymbol{u}(t),0\leq t\leq T\})$ since $\mathcal{C}_{I_i}$ is a convex set, thus any point on the line segment between $\boldsymbol{u}_i^{\rm I}$ and $\boldsymbol{u}_i^{\rm O}$ also lies in $\mathcal{C}_{I_i}$. Moreover, it can be shown that $\left(\sum_{i=1}^{\tilde{N}+1}\frac{(t_i^{\rm I}-t_{i-1}^{\rm O})^{\alpha+1}}{\alpha+1}\right)^{\frac{1}{\alpha+1}} \leq \left(\sum_{i=1}^{\tilde{N}+1}\frac{(\tilde{t}_i^{\rm I}-\tilde{t}_{i-1}^{\rm O})^{\alpha+1}}{\alpha+1}\right)^{\frac{1}{\alpha+1}} \leq \bar{f}_{{\rm O},\alpha}$ holds, since the minimum time duration for the UAV to fly between two points with horizontal locations $\boldsymbol{u}_{i-1}^{\rm O}$ and $\boldsymbol{u}_i^{\rm I}$ is achieved by letting the UAV fly in a straight path as shown in (28)–(31). This thus indicates that $(\tilde{\boldsymbol{I}},\{t_i^{\rm I},t_i^{\rm O}\}_{i=1}^{\tilde{N}},T,\{\boldsymbol{u}(t),0\leq t\leq T\})$ is a feasible solution to (P2). Furthermore, note that $T=\sum_{i=1}^{\tilde{N}+1}(t_i^{\rm I}-t_{i-1}^{\rm O})+\sum_{i=1}^{\tilde{N}}(t_i^{\rm O}-t_i^{\rm I})<\sum_{i=1}^{\tilde{N}+1}(\tilde{t}_i^{\rm I}-\tilde{t}_{i-1}^{\rm O})+\sum_{i=1}^{\tilde{N}}(\tilde{t}_i^{\rm O}-\tilde{t}_i^{\rm I})=\tilde{T}$ holds, since the minimum time duration for the UAV to fly between two points with horizontal locations $\boldsymbol{u}_{i-1}^{\rm O}$ and $\boldsymbol{u}_i^{\rm I}$, or $\boldsymbol{u}_i^{\rm I}$ and $\boldsymbol{u}_i^{\rm O}$, is achieved by letting the UAV fly in a straight path as shown in (28)–(31), which is not satisfied by the solution $(\tilde{\boldsymbol{I}},\{\tilde{t}_i^{\rm I},\tilde{t}_i^{\rm O}\}_{i=1}^{\tilde{N}},\tilde{T},\{\tilde{\boldsymbol{u}}(t),0\leq t\leq\tilde{T}\})$. Therefore, $(\tilde{\boldsymbol{I}},\{t_i^{\rm I},t_i^{\rm O}\}_{i=1}^{\tilde{N}},T,\{\boldsymbol{u}(t),0\leq t\leq T\})$ achieves a smaller objective value of (P2) compared to $(\tilde{\boldsymbol{I}},\{\tilde{t}_i^{\rm I},\tilde{t}_i^{\rm O}\}_{i=1}^{\tilde{N}},\tilde{T},\{\tilde{\boldsymbol{u}}(t),0\leq t\leq\tilde{T}\})$, which thus completes the proof of Proposition 2.

C. Proof of Proposition 3

We prove Proposition 3 by showing that for any feasible solution to (P3) denoted by $(\tilde{\boldsymbol{I}},\{\tilde{\boldsymbol{u}}_i^{\rm I},\tilde{\boldsymbol{u}}_i^{\rm O}\}_{i=1}^{\tilde{N}})$ with $\tilde{\boldsymbol{I}}=[\tilde{I}_1,...,\tilde{I}_k,...,\tilde{I}_q,...,\tilde{I}_{\tilde{N}}]^T$ and $\tilde{I}_k=\tilde{I}_q$, we can always construct an alternative solution

$(\boldsymbol{I}, \{\boldsymbol{u}_i^{\rm I}, \boldsymbol{u}_i^{\rm O}\}_{i=1}^N)$ with $\boldsymbol{I} = [I_1, ..., I_N]^T = [\tilde{I}_1, ..., \tilde{I}_k, \tilde{I}_{q+1}, ..., \tilde{I}_{\tilde{N}}]^T$ and $N = \tilde{N} - (q-k)$, which is a feasible solution to (P3) and achieves no larger objective value of (P3) compared to the solution $(\tilde{\boldsymbol{I}}, \{\tilde{\boldsymbol{u}}_i^{\rm I}, \tilde{\boldsymbol{u}}_i^{\rm O}\}_{i=1}^{\tilde{N}})$. Specifically, we set $\boldsymbol{u}_i^{\rm I} = \tilde{\boldsymbol{u}}_i^{\rm I}$ for $i = 1, ..., k$, $\boldsymbol{u}_i^{\rm I} = \tilde{\boldsymbol{u}}_{i+(q-k)}^{\rm I}$ for $i = k+1, ..., \tilde{N}-(q-k)$; and $\boldsymbol{u}_i^{\rm O} = \tilde{\boldsymbol{u}}_i^{\rm O}$ for $i = 1, ..., k-1$, $\boldsymbol{u}_i^{\rm O} = \tilde{\boldsymbol{u}}_{i+(q-k)}^{\rm O}$ for $i = k, ..., \tilde{N}-(q-k)$. Then, it can be shown that $\sum_{i=1}^{N+1} \|\boldsymbol{u}_i^{\rm I} - \boldsymbol{u}_{i-1}^{\rm O}\|^{\alpha+1} = \sum_{i=1}^{k} \|\tilde{\boldsymbol{u}}_i^{\rm I} - \tilde{\boldsymbol{u}}_{i-1}^{\rm O}\|^{\alpha+1} + \sum_{i=q+1}^{\tilde{N}+1} \|\tilde{\boldsymbol{u}}_i^{\rm I} - \tilde{\boldsymbol{u}}_{i-1}^{\rm O}\|^{\alpha+1} \leq \sum_{i=1}^{\tilde{N}+1} \|\tilde{\boldsymbol{u}}_i^{\rm I} - \tilde{\boldsymbol{u}}_{i-1}^{\rm O}\|^{\alpha+1}$ holds. Note that $(\boldsymbol{I}, \{\boldsymbol{u}_i^{\rm I}, \boldsymbol{u}_i^{\rm O}\}_{i=1}^N)$ can be easily shown to satisfy the constraints in (33)–(37), thus it is a feasible solution to (P3). Moreover, it can be shown that $\sum_{i=1}^{N+1} \|\boldsymbol{u}_i^{\rm I} - \boldsymbol{u}_{i-1}^{\rm O}\| + \sum_{i=1}^{N} \|\boldsymbol{u}_i^{\rm O} - \boldsymbol{u}_i^{\rm I}\| = \sum_{i=1}^{k} \|\tilde{\boldsymbol{u}}_i^{\rm I} - \tilde{\boldsymbol{u}}_{i-1}^{\rm O}\| + \sum_{i=q+1}^{\tilde{N}+1} \|\tilde{\boldsymbol{u}}_i^{\rm I} - \tilde{\boldsymbol{u}}_{i-1}^{\rm O}\| + \sum_{i=1}^{k-1} \|\tilde{\boldsymbol{u}}_i^{\rm O} - \tilde{\boldsymbol{u}}_i^{\rm I}\| + \|\tilde{\boldsymbol{u}}_q^{\rm O} - \tilde{\boldsymbol{u}}_k^{\rm I}\| + \sum_{i=q+1}^{\tilde{N}} \|\tilde{\boldsymbol{u}}_i^{\rm O} - \tilde{\boldsymbol{u}}_i^{\rm I}\| \overset{(C_1)}{\leq} \sum_{i=1}^{\tilde{N}+1} \|\tilde{\boldsymbol{u}}_i^{\rm I} - \tilde{\boldsymbol{u}}_{i-1}^{\rm O}\| + \sum_{i=1}^{\tilde{N}} \|\tilde{\boldsymbol{u}}_i^{\rm O} - \tilde{\boldsymbol{u}}_i^{\rm I}\|$ holds, where (C_1) can be derived by noting that $\|\tilde{\boldsymbol{u}}_q^{\rm O} - \tilde{\boldsymbol{u}}_k^{\rm I}\| = \|\sum_{i=k}^{q}(\tilde{\boldsymbol{u}}_i^{\rm O} - \tilde{\boldsymbol{u}}_i^{\rm I}) + \sum_{i=k+1}^{q}(\tilde{\boldsymbol{u}}_i^{\rm I} - \tilde{\boldsymbol{u}}_{i-1}^{\rm O})\| \leq \sum_{i=k}^{q} \|\tilde{\boldsymbol{u}}_i^{\rm O} - \tilde{\boldsymbol{u}}_i^{\rm I}\| + \sum_{i=k+1}^{q} \|\tilde{\boldsymbol{u}}_i^{\rm I} - \tilde{\boldsymbol{u}}_{i-1}^{\rm O}\|$ holds due to the triangle inequality. Therefore, $(\boldsymbol{I}, \{\boldsymbol{u}_i^{\rm I}, \boldsymbol{u}_i^{\rm O}\}_{i=1}^N)$ achieves no larger objective value of (P3) compared to the solution $(\tilde{\boldsymbol{I}}, \{\tilde{\boldsymbol{u}}_i^{\rm I}, \tilde{\boldsymbol{u}}_i^{\rm O}\}_{i=1}^{\tilde{N}})$, which thus completes the proof of Proposition 3.

D. Proof of Proposition 4

Note that with given $\boldsymbol{I}$, (P3-F) can be solved by solving $N+1$ parallel optimization problems, where each ith problem aims to minimize $\|\boldsymbol{u}_i^{\rm I} - \boldsymbol{u}_{i-1}^{\rm O}\|$ by optimizing $\boldsymbol{u}_i^{\rm I}$ and $\boldsymbol{u}_{i-1}^{\rm O}$ under the constraints in (33)–(36). For any $i \in \{2, ..., N\}$, it can be shown from the triangle inequality as well as (35) and (36) that $\|\boldsymbol{g}_{I_i} - \boldsymbol{g}_{I_{i-1}}\| = \|(\boldsymbol{u}_i^{\rm I} - \boldsymbol{u}_{i-1}^{\rm O}) + (\boldsymbol{u}_{i-1}^{\rm O} - \boldsymbol{g}_{I_{i-1}}) + (\boldsymbol{g}_{I_i} - \boldsymbol{u}_i^{\rm I})\| \leq \|\boldsymbol{u}_i^{\rm I} - \boldsymbol{u}_{i-1}^{\rm O}\| + \|\boldsymbol{u}_{i-1}^{\rm O} - \boldsymbol{g}_{I_{i-1}}\| + \|\boldsymbol{u}_i^{\rm I} - \boldsymbol{g}_{I_i}\| \leq \|\boldsymbol{u}_i^{\rm I} - \boldsymbol{u}_{i-1}^{\rm O}\| + 2\bar{d}$ holds, which implies that $\|\boldsymbol{u}_i^{\rm I} - \boldsymbol{u}_{i-1}^{\rm O}\| \geq \max\{\|\boldsymbol{g}_{I_i} - \boldsymbol{g}_{I_{i-1}}\| - 2\bar{d}, 0\}$ holds due to the non-negativeness of norm functions. Similarly, it can be shown that $\|\boldsymbol{u}_0 - \boldsymbol{g}_{I_1}\| = \|(\boldsymbol{u}_0^{\rm O} - \boldsymbol{u}_1^{\rm I}) + (\boldsymbol{u}_1^{\rm I} - \boldsymbol{g}_{I_1})\| \leq \|\boldsymbol{u}_1^{\rm I} - \boldsymbol{u}_0^{\rm O}\| + \bar{d}$ and $\|\boldsymbol{u}_F - \boldsymbol{g}_{I_N}\| = \|(\boldsymbol{u}_{N+1}^{\rm I} - \boldsymbol{u}_N^{\rm O}) + (\boldsymbol{u}_N^{\rm O} - \boldsymbol{g}_{I_N})\| \leq \|\boldsymbol{u}_{N+1}^{\rm I} - \boldsymbol{u}_N^{\rm O}\| + \bar{d}$ hold, which implies that $\|\boldsymbol{u}_1^{\rm I} - \boldsymbol{u}_0^{\rm O}\| \geq \max\{\|\boldsymbol{u}_0 - \boldsymbol{g}_{I_1}\| - \bar{d}, 0\}$ and $\|\boldsymbol{u}_{N+1}^{\rm I} - \boldsymbol{u}_N^{\rm O}\| \geq \max\{\|\boldsymbol{u}_F - \boldsymbol{g}_{I_N}\| - \bar{d}, 0\}$ hold. By further noting that the solution in (43)–(46) yields $\|\boldsymbol{u}_i^{\rm I} - \boldsymbol{u}_{i-1}^{\rm O}\| = \max\{\|\boldsymbol{g}_{I_i} - \boldsymbol{g}_{I_{i-1}}\| - 2\bar{d}, 0\}$, $\forall i \in \{2, ..., N\}$, $\|\boldsymbol{u}_1^{\rm I} - \boldsymbol{u}_0^{\rm O}\| = \max\{\|\boldsymbol{u}_0 - \boldsymbol{g}_{I_1}\| - \bar{d}, 0\}$, and $\|\boldsymbol{u}_{N+1}^{\rm I} - \boldsymbol{u}_N^{\rm O}\| = \max\{\|\boldsymbol{u}_F - \boldsymbol{g}_{I_N}\| - \bar{d}, 0\}$, the optimal value of (P3-F) with given $\boldsymbol{I}$ is given in (42), which thus completes the proof of Proposition 4.

REFERENCES

[1] S. Zhang, Y. Zeng, and R. Zhang, "Cellular-enabled UAV communication: A connectivity-constrained trajectory optimization perspective," *IEEE Trans. Commun.*, Early Access. [Online]. Available: https://arxiv.org/abs/1805.07182.

[2] B. V. D. Bergh, A. Chiumento, and S. Pollin, "LTE in the sky: Trading off propagation benefits with interference costs for aerial nodes," *IEEE Commun. Mag.*, vol. 54, no. 5, pp. 44–50, May 2016.

[3] X. Lin *et al.*, "The sky is not the limit: LTE for unmanned aerial vehicles," *IEEE Commun. Mag.*, vol. 56, no. 4, Apr. 2018.

[4] 3GPP TR 36.777, "Enhanced LTE support for aerial vehicles (release 15)," V15.0.0.

[5] Y. Zeng, J. Lyu, and R. Zhang, "Cellular-connected UAVs: Potentials, challenges and promising technologies," *IEEE Wireless Commun.*, Early Access. [Online]. Available: https://arxiv.org/abs/1804.02217.

[6] L. Liu, S. Zhang, and R. Zhang, "Multi-beam UAV communication in cellular uplink: Cooperative interference cancellation and sum-rate maximization," [Online]. Available: https://arxiv.org/abs/1808.00189, Jul. 2018.

[7] ——, "Exploiting NOMA for multi-beam UAV communication in cellular uplink," [Online]. Available: https://arxiv.org/abs/1810.10839, Oct. 2018.

[8] W. Mei, Q. Wu, and R. Zhang, "Cellular-connected UAV: Uplink association, power control and interference coordination," [Online]. Available: https://arxiv.org/abs/1807.08218, Jul. 2018.

[9] W. Mei and R. Zhang, "Uplink cooperative NOMA for cellular-connected UAV," [Online]. Available: https://arxiv.org/abs/1809.03657, Sep. 2018.

[10] M. Mozaffari, A. T. Z. Kasgari, W. Saad, M. Bennis, and M. Debbah, "Beyond 5G with UAVs: Foundations of a 3D wireless cellular network," *IEEE Trans. Wireless Commun.*, Early Access. [Online]. Available: https://arxiv.org/abs/1805.06532.

[11] E. Bulut and I. Guvenc, "Trajectory optimization for cellular-connected UAVs with disconnectivity constraint," in *Proc. IEEE Int. Conf. Commun. (ICC) Wkshps.*, May 2018.

[12] A. J. Goldsmith, *Wireless Communications*. Cambridge Univ. Press, 2005.

[13] S. Kaul, R. Yates, and M. Gruteser, "Real-time status: How often should one update?" in *Proc. IEEE Int. Conf. Comput. Commun. (INFOCOM)*, Jun. 2012.

[14] D. B. West, *Introduction to Graph Theory*. Prentice Hall, 2001.

[15] M. Grant and S. Boyd, "CVX: Matlab software for disciplined convex programming," version 2.1. [Online]. Available: http://cvxr.com/cvx/, Jun. 2015.

[16] M. S. Lobo, L. Vandenberghe, S. Boyd, and H. Lebret, "Applications of second-order cone programming," *Linear Algebra Applicat.*, vol. 284, no. 1-3, pp. 193–228, Nov. 1998.

[17] W. H. Freeman, *Computers and Intractability: Guide to the Theory of NP-Completeness*. New York, 1979.

[18] G. Y. Handler and I. Zang, "A dual algorithm for the constrained shortest path problem," *Networks*, vol. 10, pp. 293–310, 1980.

[19] A. Jüttner, B. Szviatovszki, I. Mecs, and Z. Rajko, "Lagrange relaxation based method for the QoS routing problem," in *Proc. IEEE Int. Conf. Comput. Commun. (INFOCOM)*, Jun. 2001.

[20] J. Y. Yen, "Finding the k shortest loopless paths in a network," *Manag. Science*, vol. 17, no. 11, pp. 712–716, 1971.

[21] S. Boyd and L. Vandenberghe, *Convex Optimization*. Cambridge Univ. Press, 2004.

[22] A. Jüttner, "On resource constrained optimization problems," in *Proc. 4th Japanese-Hungarian Symp. Discr. Math. Appl.*, 2005.

[23] W. B. Powell, *Approximate Dynamic Programming: Solving the Curses of Dimensionality*. John Wiley & Sons, 2007.